Electronic Theses and Dissertations

Theses, Dissertations, and Major Papers

11-29-2018

Investigation on Lean NOx Trap Regeneration Using Alcohol Fuels

Divyanshu Purohit
University of Windsor

Follow this and additional works at: https://scholar.uwindsor.ca/etd

Investigation on Lean NO$_x$ Trap Regeneration Using Alcohol Fuels

by

Divyanshu Purohit

A Thesis
Submitted to the Faculty of Graduate Studies
through Mechanical, Automotive, and Materials Engineering
in Partial Fulfillment of the Requirements for
the Degree of Master of Applied Science at the
University of Windsor

Windsor, Ontario, Canada

Investigation on Lean NO$_x$ Trap Regeneration Using Alcohol Fuels

by

Divyanshu Purohit

APPROVED BY:

_____
X. Chen
Department of Electrical and Computer Engineering

_____
N. Eaves
Department of Mechanical, Automotive, and Materials Engineering

_____
M. Zheng, Advisor
Department of Mechanical, Automotive, and Materials Engineering

29th November 2018

AUTHOR'S DECLARATION OF ORIGINALITY

I hereby certify that I am the sole author of this thesis and that no part of this thesis has been published or submitted for publication.

I certify that, to the best of my knowledge, my thesis does not infringe upon anyone's copyright nor violate any proprietary rights and that any ideas, techniques, quotations, or any other material from the work of other people included in my thesis, published or otherwise, are fully acknowledged in accordance with the standard referencing practices. Furthermore, to the extent that I have included copyrighted material that surpasses the bounds of fair dealing within the meaning of the Canada Copyright Act, I certify that I have obtained a written permission from the copyright owner(s) to include such material(s) in my thesis and have included copies of such copyright clearances to my appendix.

I declare that this is a true copy of my thesis, including any final revisions, as approved by my thesis committee and the Graduate Studies office, and that this thesis has not been submitted for a higher degree to any other University or Institution.

ABSTRACT

The impacts of automotive pollutants on local air quality, human health, and climate change are a major concern worldwide. Therefore, the internal combustion engine (ICE) powered automobiles are expected to be able to meet the increasingly stringent emission and fuel efficiency standards. The reduction in oxides of nitrogen (NO_x) in lean burn and diesel-fueled compression ignition (CI) engines is a major challenge.

In this research, the use of alcohol fuel such as n-butanol and ethanol is studied in a CI engine. With the application of moderate exhaust gas recirculation (EGR), low engine-out NO_x and soot emissions are achieved simultaneously. However, to meet NO_x emission regulations, the use of only alternative fuels is not sufficient for a wide range of engine operating conditions. Therefore, lean NO_x trap (LNT) after-treatment system is used for further NO_x reduction using a reductant. In this study, an investigation on the performance of long breathing LNT is performed using ethanol, n-butanol, and diesel as reductants. The LNT regeneration experiments are conducted on a heated flow bench under simulated engine exhaust like conditions. Ethanol and n-butanol are found to be more effective compared to diesel as a reductant in terms of NO_x conversion, ammonia (NH_3) slip, nitrogen dioxide (N_2O) slip, and hydrogen (H_2) formation, during the LNT regeneration period at the tested conditions. The formation of NH_3 and N_2O during the LNT regeneration is not desired. Albeit, the NH_3 generated during the LNT regeneration can be utilized to further reduce NO_x using a selective catalytic reduction (SCR) convertor downstream of the LNT catalyst. In this study, the combined LNT-SCR tests are performed to investigate overall NO_x reduction using n-butanol as a reductant.

DEDICATION

This work is dedicated to my parents and sister.

I couldn't be where I am today without you.

ACKNOWLEDGEMENTS

TABLE OF CONTENTS

LIST OF FIGURES

LIST OF TABLES

LIST OF NOMENCLATURE

Abbreviations

AMOx	Ammonia Oxidation Catalyst	[-]
ANR	Ammonia to NO_x ratio	[-]
AVL	Anstalt für Verbrennungskraftmaschinen List	[-]
ATR	Auto-thermal Reforming	[-]
CA	Crank Angle	[°]
CA50	Crank Angle of 50% Cumulative Heat Release	[°CA]
CAI	California Analytical Instruments	[-]
CARB	California Air Resources Board	[-]
CI	Compression Ignition	[-]
CLD	Chemiluminescence Detector	[-]
CCEL	Clean Combustion Engine Lab	[-]
CNG	Compressed Natural Gas	[-]
DEF	Diesel Exhaust Fluid	[-]
DI	Direct Injection	[-]
DME	Dimethyl Ether	[-]
DOC	Diesel Oxidation Catalyst	[-]
DPF	Diesel Particulate Filter	[-]
DR	Dry Reforming	[-]
EGR	Exhaust Gas Recirculation	[-]
EPA	Environmental Protection Agency	[-]
FPGA	Field Programmable Gate Array	[-]
FTIR	Fourier Transform Infrared Spectrometer	[-]
GHG	Greenhouse Gas	[-]
HCCI	Homogenous Charge Compression Ignition	[-]
HDD	Heavy-Duty Diesel	[-]
HFID	Heated Flame Ionization Detector	[-]

HFRR	High-Frequency Reciprocating Rig	[-]
HSV	Hourly Space Velocity	[hr^{-1}]
ICE	Internal Combustion Engine	[-]
IMEP	Indicated Mean Effective Pressure	[bar]
LNG	Liquid Natural Gas	[-]
LNT	Lean NO$_x$ Trap	[-]
LPG	Liquefied Petroleum Gas	[-]
LTC	Low Temperature Combustion	[-]
MAF	Mass Air Flow	[g/s]
NDIR	Nondispersive Infrared	[-]
NI	National Instruments	[-]
NSR	NO$_x$ Storage and Reduction	[-]
p_{inj}	Injection Pressure	[bar]
PM	Particulate Matter	[-]
ppm	Parts Per Million	[ppm]
PFI	Port Fuel Injection	[-]
PWM	Pulse Width Modulation	[-]
SCR	Selective Catalytic Reduction	[-]
SI	Spark Ignition	[-]
SR	Steam Reforming	[-]
TWC	Three-Way Catalyst	[-]
UHC	Unburned Hydrocarbon	[-]
WGS	Water Gas Shift	[-]

Chemical Formulae

Al_2O_3	Aluminum Oxide
Ba	Barium
$BaCO_3$	Barium Carbonate
$Ba(NO_2)_2$	Barium Nitrite

$Ba(NO_3)_2$	Barium Nitrate
BaO	Barium Oxide
C_3H_6	Propene
C_2H_6O	Ethanol
$C_4H_{10}O$	Butanol
CH_4	Methane
$CO(NH_2)_2$	Urea
CO	Carbon Monoxide
CO_2	Carbon Dioxide
H_2	Hydrogen
H_2O	Water
NO_x	Oxides of Nitrogen
N_2O	Nitrous Oxide
NH_3	Ammonia
NO	Nitric Oxide
NO_2	Nitrogen Dioxide
N_2	Nitrogen
O_2	Oxygen
Pt	Platinum
Pd	Palladium
Rh	Rhodium

CHAPTER 1:   INTRODUCTION

Internal Combustion (IC) engines, specifically spark ignition (SI) and compression ignition (CI) engines, have been used extensively in the transportation sector. Diesel engines are widely used for the heavy-duty applications because of high efficiency, torque characteristics, mechanical reliability, and robustness. Diesel engines have the inherent benefits of higher fuel efficiency and lower carbon dioxide (CO_2) emissions compared to the conventional gasoline engines [1-4]. However, the production of harmful emissions from diesel vehicles is a serious drawback. The continuously increasing demand for the reductions in exhaust emissions and fuel consumption without compromising the engine performance has been a challenge. In this chapter research motivation, background information and engineering challenges associated with the research objectives are presented. An overview of the currently used emission reduction technologies has been provided followed by the thesis structure at the end.

1.1 Research Motivation

Raw exhaust from the modern diesel engines contains excess air, along with combustion products such as CO_2, water (H_2O) and pollutants. Major pollutants in the diesel engine exhaust gases include oxides of nitrogen (NO_x), particulate matter (PM), unburned or partially burned hydrocarbons, carbon monoxide (CO), and greenhouse gases (GHG). The relative volumetric concentrations of pollutants in typical modern diesel engine exhaust gases are shown in Figure 1-1 [3]. Despite being lower in relative concentration, those pollutants are harmful to human health and the environment. In 2010, heavy-duty trucks and buses mostly powered by the diesel engines accounted for more than 80% of global PM and NO_x emissions from on-road vehicles [4].

1
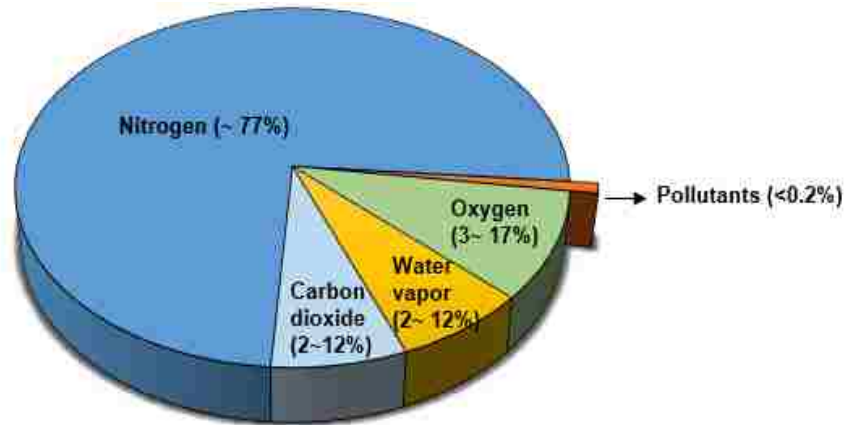
Figure 1-1: Relative concentration of pollutants in modern diesel engine exhausts [3]

The combustion processes in conventional diesel engines are often summarized in 4 stages: Ignition delay, premixed burn, diffusion burn, and the burning-up tail [1-3]. Diesel engine combustion occurs in a heterogeneous mixture of air and fuel, in which fuel is injected into the cylinder to initiate the combustion. The formation of pollutants during the combustion process is strongly affected by the atomization and mixing of fuel droplets into the air.

The NO_x formation depends on the temperature of the flame front or burning sites, oxygen (O_2) concentration, and residence time during the combustion process [1,2]. The NO_x formation aggravates when the high temperature burning zones are compressed under high temperature and pressure conditions [1-3]. In conventional diesel engines when the flame temperatures are in excess of 2200 K, the thermal NO_x mechanism described by the extended Zeldovich mechanism is responsible for the majority of NO_x emissions [1,5]. The elevated temperatures and O_2 concentration results in high NO formation rates.

With the rising number of vehicles on the road every day, the air quality has become a significant concern for the society and environments. The NO_x is considered as a precursor of photochemical smog, which is a significant form of air pollution because of the adverse effect on human health and environments. The presence of NO_x in atmosphere also tends

2

to form nitric acid, which contributes to acid rain. In order to minimize the effects on environments, emission regulatory authorities such as California Air Resources Board (CARB) and Environmental Protection Agency (EPA) of the United States, have been continuously tightening the emission standards over the past decades. Initially, when the emission regulations were implemented between 1998 to 2006, the authorities such as EPA had focused on the NO_x reduction. However, starting from 2007, PM emission limits became stringent, and vehicle manufacturers had to use diesel particulate filter (DPF) to meet the emission certification limits [6]. Currently, the NO_x and PM emission limits regulated by the United States EPA for heavy-duty vehicles are 0.27 g/kW·hr and 0.013 g/kW·hr respectively. During meantime the European Union has tightened the NOx and PM emissions similarly. The trends of NO_x and PM emission certification limits for heavy-duty diesel vehicles set by the EPA and EU are shown in Figure 1-2.
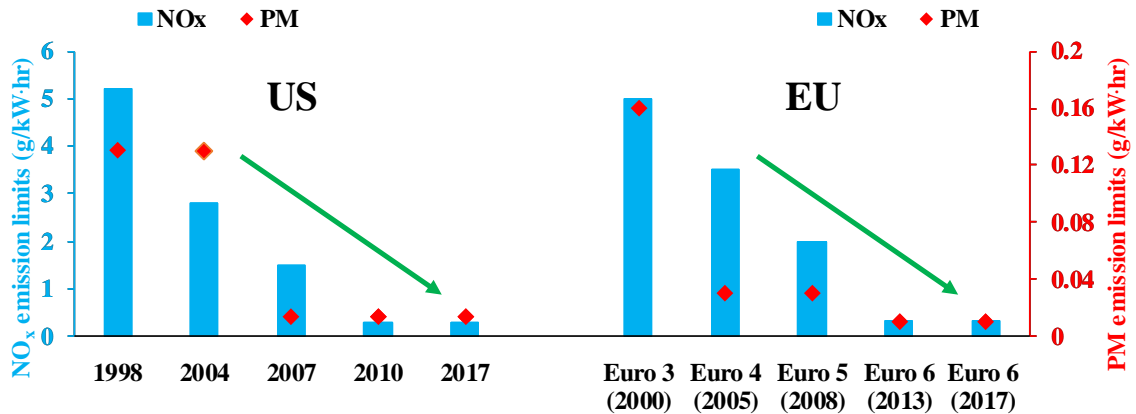
Figure 1-2: Heavy-duty diesel emission standards [7,8]

Compared with previous standards [6-8], emission regulations are trending towards near zero levels. Reduction in emissions to achieve the current and future emission standards may not be quite possible by only using advanced internal combustion strategies. Therefore, the use of an exhaust after-treatment system is imperative to meet the current

3

and future stringent emission regulations. The reductions in NO_x emissions can be achieved using two pathways: in-cylinder techniques and exhaust gas after-treatment systems, which are discussed further.

1.2 In-cylinder NO_x Reduction Approaches

In-cylinder techniques have been implemented and investigated extensively for the emission reduction from CI engines. The use of exhaust gas recirculation (EGR), alternative fuels, fuel injection control for delayed combustion phasing, and advanced combustion strategies such as low-temperature combustion (LTC) for NO_x reduction have been investigated by the researchers [9-22,26,27].

EGR is a well-established method for the in-cylinder NO_x reduction. When EGR is applied, a certain fraction of the engine exhaust gas is recirculated into the engine intake manifold, where it mixes with the fresh charge. By large, an exhaust gas mainly comprises of nitrogen (N_2), CO_2 and H_2O. The recirculated exhaust gas decreases the specific heat capacity ratio of the air-fuel mixture for combustion [1,2]. As a result, the in-cylinder flame temperature is decreased, which reduces the NO_x formation during the combustion. Ladomatos *et al*. demonstrated the dilution, thermal, and chemical effects of EGR on NO_x emissions [9,10]. The effect of in-cylinder O_2 concentrations on the flame temperatures were reported to be most influential on NO_x and PM formation [9]. In comparison, it was found that the dilution effect was in dominance compared with the thermal and chemical effects of EGR [10]. The high flame temperatures, in conventional high-temperature combustion (HTC) diesel engines result in high NO_x formation, under the O_2 and N_2 abundant environment [10]. Several other studies have demonstrated that the use of EGR reduces the NO_x emissions [11-14].

4

Simultaneously high NO_x and PM emissions are inevitable in the HTC [14]. The effect of EGR dilution on NO_x and PM emissions can be seen in Figure 1-3, as an example for diesel combustion. The application of EGR results in the well-known classical HTC trade-off between NO_x and PM emissions [9-14]. With the increase in EGR, the NO_x decreases, while the PM tends to increase. The PM formation increases because of the predominant diffusion-controlled combustion, where the reduction in O_2 abundancy leads to the elevated PM formation [15].

However, when a use of heavy EGR (i.e. 9-11% intake O_2) is applied, the PM decreases as shown in Figure 1-3. This region of simultaneously low NO_x and PM emissions is termed as LTC region. However, a major drawback under the LTC region is the increase in CO and THC emissions indicating a reduction in combustion efficiency. The effect of EGR on CO and THC emissions is shown in Figure 1-4. The increase in CO and THC emissions is significant under the LTC region. Therefore, under LTC region a trade-off can be recognized, that is, the CO and HC vs the NO_x and PM [14].
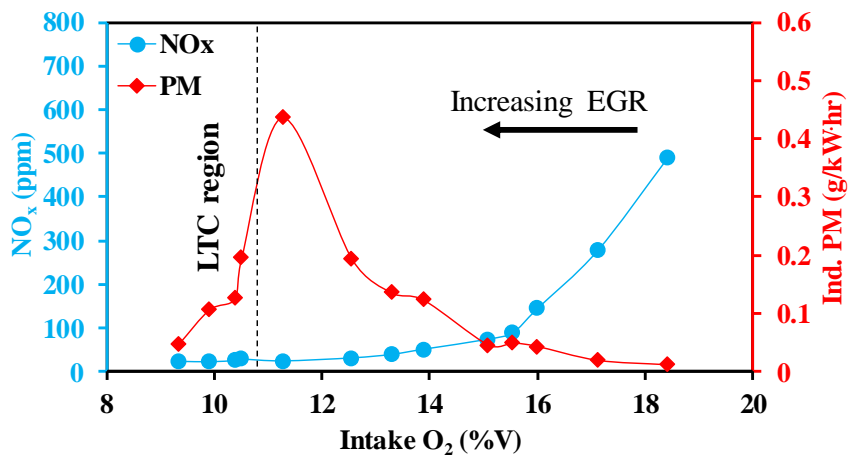
Figure 1-3: Effect of EGR on NO_x and PM emissions
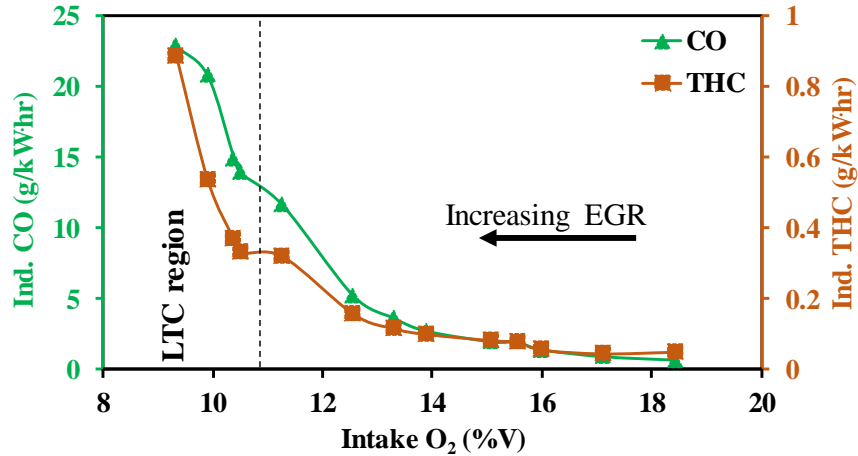
Figure 1-4: Effect of EGR on CO and THC emissions

An extensive amount of research has been carried out on the diesel LTC because of the simultaneous low NO_x and PM emissions [14,16-20]. Under the LTC mode, the flame temperature is reduced with the application of heavy EGR. Thus, the ignition delay is prolonged that results in premixed combustion and decreased PM formation [21,22]. Zheng *et al*. reported that catalytic reforming of EGR can be used to partially reform the exhaust gas to improve the cycle to cycle variation and combustion stability during LTC. The study also demonstrated that the NO_x emissions were reduced by the application of catalytic EGR compared to raw EGR [20].

The use of alternative fuels in IC engines can also help in reducing the emissions during combustion. Commercially diesel and gasoline fuel are widely used in the transportation sector because of their high volumetric energy density. Nevertheless, there are other potential bio-fuels as well, which could be utilized to power the automobiles. The ethanol produced from sugarcane reduces the GHG emissions by 40% to 62% compared to the gasoline [23]. Since 2015, the government of Brazil has set the mandatory rule for 27% ethanol blend in gasoline to reduce emissions from the transportation sector [24]. The United States EPA also has set regulations for 10% ethanol blend in the gasoline [25].

Since, diesel fuel is not suitable for a wide range of load under LTC mode due to its high viscosity and boiling temperature leading to longer mixing time, and higher CO and THC emissions [18]. The alcohol fuels such as ethanol and n-butanol have lower boiling points than diesel. The lower boiling point of fuel helps in the improved air and fuel mixing, and higher latent heat of vaporization of fuel decreases the combustion temperature. Additionally, alcohol fuels have lower CO_2 emissions because they can be derived from biomass [23].

Yanai *et al*. investigated the direct injection of neat n-butanol in a diesel engine without application of EGR and reported that low NO_x and soot emissions could be achieved, but load range was limited due to unstable combustion [26]. Gao *et al*. demonstrated the effect of diesel direct injection (DI) with ethanol port fuel injection (PFI) strategies for simultaneous low NO_x and soot emissions [27]. The alcohol fuels, such as ethanol and n-butanol have higher O_2 content in fuel and higher volatility that have been found to be beneficial for achieving low NO_x and PM emissions [18]. Even with the use of alternative fuels and advanced combustion modes, exhaust after-treatment systems are required to meet the current and future emission regulations under wide engine operating conditions.

1.3 Exhaust After-treatment Systems

The after-treatment systems in combination with in-cylinder emission reduction strategies have become an important aspect to meet the progressive reduction in emissions. The after-treatment devices include filters and catalytic converters that help in the reduction of engine-out emissions. The use of these exhaust after-treatment devices also allows improvement in the engine performance for a wide range of operation. However, the continuous variation in the exhaust temperature and the gas concentration affects the

performance of an after-treatment system. Therefore, advanced after-treatment systems are required to curb the emissions for a wide range of engine operating conditions. A conventional aftertreatment system configuration used on diesel-fuelled vehicles for emission reduction is shown in Figure 1-5.
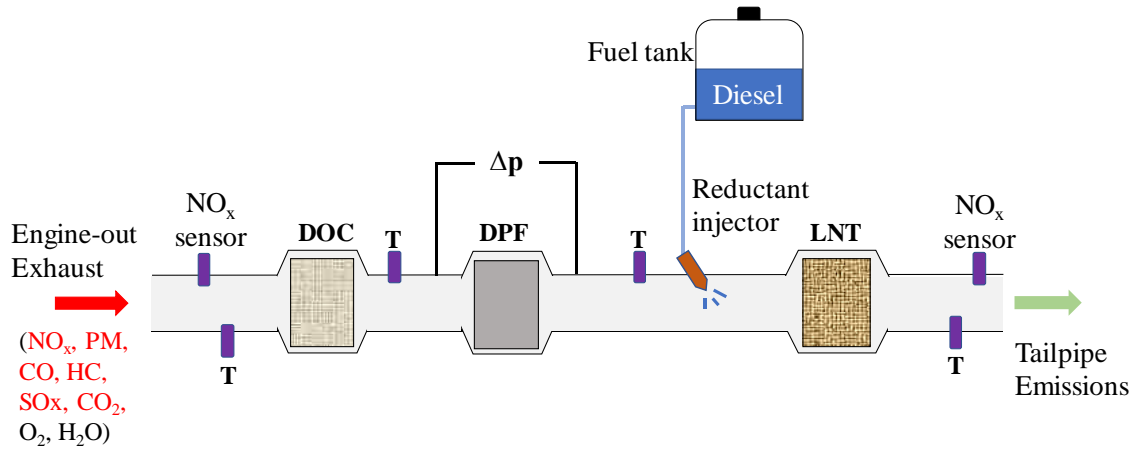
Figure 1-5: Conventional after-treatment system in diesel vehicle

Role of Diesel Oxidation Catalyst and Diesel Particulate Filter

Diesel oxidation catalyst (DOC) consists of honeycomb structured ceramic monoliths impregnated with precious group metals (PGM) (e.g. Platinum (Pt) and Palladium (Pd)). The primary purpose of the DOC in diesel exhaust after-treatment system is the oxidation of unburned HC and CO [28]. In same application DOC also oxidizes NO to NO_2, and this NO_2 promotes soot oxidation on the diesel particulate filter (DPF) [28,29].

A DPF is an exhaust after-treatment device that filters and stores the PM emissions from the engine-out exhaust. Since 2010, DPF has become an essential device and is used in every modern diesel-fuelled vehicle to meet the PM emissions limits [30,31]. Commonly ceramic or metallic wall-through filters are used commercially depending on the applications. It has been reported in literatures that DPF filtration efficiency can reach up

to 99% for monolith wall through filters [30]. Over an operating period, soot and ash layers gets accumulated on the walls of a filter, which increases the engine back pressure. Therefore, the removal of soot and ash from DPF is necessary. Soot, unlike ash, is a combustible material. Periodically, HC is injected into the exhaust to oxidize the soot on DPF. Commercial diesel is often used to regenerate the DPF during active regeneration. During passive regeneration, oxidation reactions occurs by NO_2 under the standard exhaust conditions, and in active regeneration changes are made in exhaust conditions through HC injection. The ash could be potentially removed by cleaning during maintenance [32].

Lean Burn Exhaust After-treatment Systems for NO_x Reduction

In-cylinder strategies can reduce the NO_x emissions to a certain extent, and after-treatment systems are required to further reduce the engine-out NO_x. The urea-based selective catalytic reduction (SCR) and lean NO_x trap (LNT) are two well-established technologies used in the transportation sector for NO_x reduction under lean engine operating conditions.

Selective Catalytic Reduction

The urea-based SCR is a NO_x reduction technology that uses ammonia as reductant over the SCR convertor. This technology can achieve higher NO_x conversion under lean burn conditions. The SCR after-treatment system needs aqueous urea $((NH_2)_2CO)$ solution also known as DEF (Diesel Exhaust Fluid) or Ad-Blue, which provides ammonia (NH_3) on decomposition in exhaust [33,34]. Diesel vehicles are equipped with an urea delivery system for SCR. A typical urea delivery system consists of a storage tank, heater, sensors, doser, pump, and dosing control module that controls dosing the required amount of DEF

for NO_x reduction independent of engine control [34]. The quantity of urea required for the NO_x reduction is generally calculated based on the engine out NO_x emissions.

Aqueous urea solution often contains 32.5% urea and deionized water in balance. This composition of urea and water provides a freezing temperature of -11°C, which is required during cold weather conditions [34]. The urea injected into hot exhaust produces ammonia (NH_3) because of the thermolysis and hydrolysis effects [34]. The performance of SCR depends on the vaporization and proper mixing of injected aqueous urea solution. When urea is used as a reducing agent, the reaction pathways involved in NO_x reduction are: urea hydrolysis (Equation 1.1) to NH_3; standard reaction (Equation 1.2) when NO is present alone; and fast SCR reaction (Equation 1.3) when both NO and NO_2 are present; and slow reaction (Equation 1.4) when only NO_2 is present [34].

$$(NH_2)_2CO + H_2O \leftrightarrow 2NH_3 + CO_2 \qquad \text{(Equation 1.1)}$$

$$NH_3 + NO + \frac{1}{4}O_2 \rightarrow N_2 + \frac{3}{2}H_2O \qquad \text{(Equation 1.2)}$$

$$NH_3 + \frac{1}{2}NO + \frac{1}{2}NO_2 \rightarrow N_2 + \frac{3}{2}H_2O \qquad \text{(Equation 1.3)}$$

$$NH_3 + \frac{3}{4}NO_2 \rightarrow \frac{7}{8}N_2 + \frac{3}{2}H_2O \qquad \text{(Equation 1.4)}$$
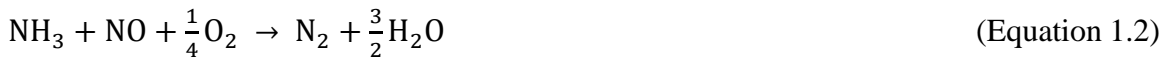
The urea-based SCR after-treatment technology is well established and can achieve high NO_x conversion efficiency [34]. However, there are some glitches that need to be resolved to improve this technology. Some shortcomings of urea-based SCR technology addressed by previous researchers are: the limited NO_x conversion at low-load driving conditions (vanadium SCR catalyst) [35], sensitivity towards sulfation (copper SCR catalyst) [36], and ammonia slip and urea crystallization in urban driving condition, i.e. when the exhaust

temperature is below 200°C for light-duty, whereas urea requires 180°C to vaporize into NH$_3$ [37,38]. The urea-based SCR system requires additional distribution infrastructure for periodic refills, packaging for on-board urea storage, heating and injection system with complex control strategies. This increases the overall cost of a vehicle. A wide range of engine operating conditions requires continuous dosing of DEF in the exhaust stream for efficient NO$_x$ conversion. Sometimes this leads to a slip of ammonia into the environment [34]. NH$_3$ is poisonous and harmful in high concentration for the environment. Therefore, Heavy-duty diesel vehicles are also equipped with an ammonia oxidation catalyst (AMOx) downstream of SCR to avoid excessive NH$_3$ slip from the tailpipe [34].

Lean NO$_x$ Trap

The lean NO$_x$ trap (LNT) or NO$_x$ storage and reduction (NSR) catalyst are exhaust after-treatment technologies for the NO$_x$ reduction from lean burn engine exhaust. Since the 1990s, LNT or NSR catalyst has been investigated [39,40]. An LNT catalyst is mostly used in passenger cars and light duty trucks. An LNT catalyst operates on periodic lean and rich operations, also termed as adsorption and regeneration periods, respectively. The NO$_x$ is stored during the adsorption period on an LNT catalyst. Then during the LNT regeneration, the stored NO$_x$ is reduced with the help of reducing agents [39,40]. A representative case for an LNT operation cycle (adsorption and regeneration) is shown in Figure 1-6 as an example.
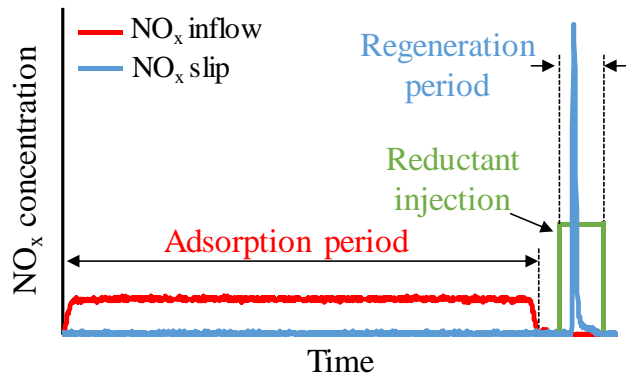
Figure 1-6: Adsorption and regeneration periods during an LNT operation

The engine-out NO_x formed during engine operation is absorbed on the storage sites of an LNT catalyst. Initially, during the adsorption period, the catalytic oxidation of NO to NO_2 occurs on the PGM sites. The NO_x is trapped on the catalyst in the form of nitrites and nitrates because of the oxidation reactions. The NO_x storage reactions on an LNT catalyst are shown in Equation 1.4 and 1.5. The storage sites on the LNT catalyst gradually saturates, as the engine-out NO_x gets adsorbed on it during the lean period. For instance, the duration of the adsorption period in conventional LNT operation is 60 seconds on certain operating conditions. The NO_x adsorption process on an LNT catalyst surface is shown schematically in Figure 1-7.
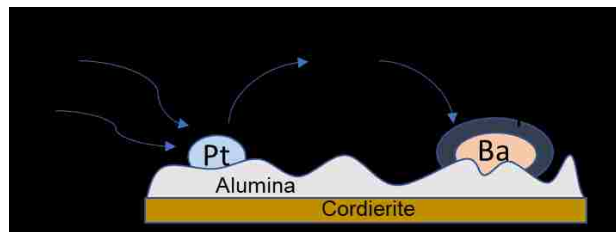
Figure 1-7: NO_x adsorption on LNT catalyst, adapted from [41]

$$BaCO_3 + 2NO_2 + \frac{1}{2}O_2 \longrightarrow Ba(NO_3)_2 + CO_2 \qquad \text{(Equation 1.4)}$$

$$BaCO_3 + 2NO + \frac{3}{2}O_2 \longrightarrow Ba(NO_3)_2 + CO_2 \qquad \text{(Equation 1.5)}$$
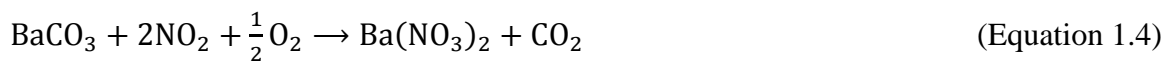
During the regeneration period, a reductant (e.g. HC, H_2 or CO) is introduced upstream of the LNT catalyst into the exhaust stream by either in-cylinder post injection or local exhaust pipe injection. This leads to an O_2 deficiency in the exhaust mixture. The injection of reductant initiates the regeneration reactions on the LNT catalyst. The stored NO_x is reduced, but some portion slips, producing an unreduced spike. The alcohol fuels such as ethanol and n-butanol can also be used for the LNT regeneration. The NO_x reduction process on the LNT catalyst surface is shown in Figure 1-8. The LNT regeneration involves complex chemical reaction mechanisms. Some of the LNT regeneration reactions are as follows:

$$Ba(NO_3)_2 + \frac{5}{9}C_3H_6 \rightarrow N_2 + BaO + \frac{5}{3}CO_2 + \frac{5}{3}H_2O \qquad \text{(Equation 1.6)}$$

$$Ba(NO_3)_2 + 8H_2 \rightarrow 2NH_3 + BaO + 5H_2O \qquad \text{(Equation 1.7)}$$

$$Ba(NO_3)_2 + 3CO \longrightarrow BaCO_3 + 2NO + 2CO_2 \qquad \text{(Equation 1.8)}$$

$$Ba(NO_3)_2 + 3H_2 + CO_2 \longrightarrow BaCO_3 + 2NO + 3H_2O \qquad \text{(Equation 1.8)}$$
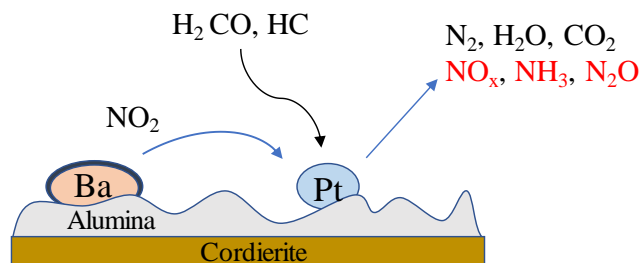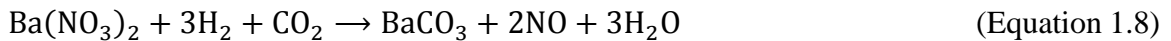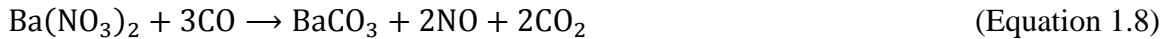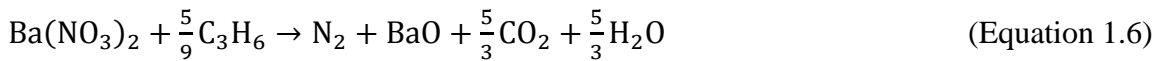
Figure 1-8: NO_x reduction on LNT catalyst, adapted from [41]

Generally, the active control for the LNT regeneration is used on the vehicles, in which the fuel as a reductant is injected into the exhaust periodically to reduce the stored NO_x. Therefore, the overall fuel consumption of a vehicle increases. The LNT technology has

drawbacks such as higher cost of production due to PGM's and inconsistent NO_x conversion efficiency. However, the LNT technology has advantages over the urea-based SCR system such as lower cost (for light-duty), on-board fuel can be used as reducing agent, requires less complex control strategy and hardware packaging. Therefore, in this research, an LNT after-treatment system is investigated. To meet the current and future stringent NO_x emission regulations, an LNT is also being used with a SCR on the vehicles [42].

Long Breathing Strategy for Lean NO_x Trap

The long breathing strategy is developed to reduce tailpipe NO_x emission by combining in-cylinder NO_x reduction with an LNT after-treatment system [43-45]. The use of EGR helps in reducing the NO_x formation as discussed earlier. In the long breathing strategy for an LNT operation, the NO_x adsorption period is prolonged as a result of the reduced engine-out NO_x levels [43,44]. Accordingly, lesser LNT regeneration periods are required compared to the conventional LNT operation, which requires frequent regenerations [43-45]. A representative case for conventional LNT and long breathing LNT operation is shown in Figures 1-9 and 1-10. Higher engine-out NO_x emissions would otherwise saturate the storage sites on the LNT at a faster rate. Consequentially, frequent regenerations are required. The use of long breathing strategy reduces the fuel penalty associated with the LNT regeneration [43-45]. The engine-out NOx emission limits for long breathing LNT operation has been proposed to be 100 ppm [44,45].

The PM emissions increases with the application of EGR. A DPF is used to filter the PM from the exhaust. The higher PM emissions can saturate a DPF fast, and frequent HC injections will be required to oxidize the soot on a DPF, which increases the fuel penalty

14

associated with a DPF. Modern heavy-duty diesel (HDD) vehicles are equipped with a DPF to meet the current PM emission limit of 0.013 g/kW·hr. Considering DPF filtration efficiency of 90 to 95%, the indicated PM emission limit suitable for long breathing LNT has been proposed to be 0.1 g/kW·hr [44]. Both NO_x and PM emissions should be below the mentioned limits simultaneously for long breathing LNT operations.
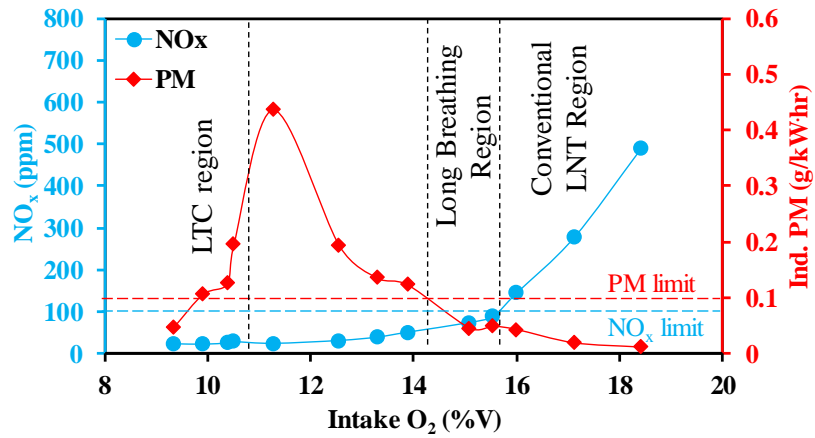
Figure 1-9: Conventional LNT and long breathing LNT operation regions
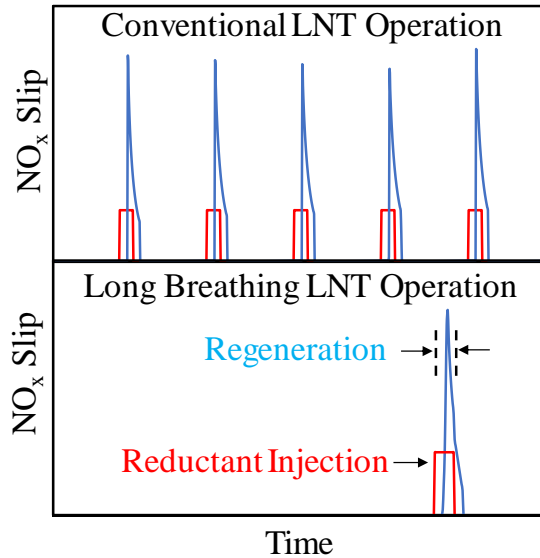
Figure 1-10: Comparison between conventional and long breathing LNT

1.4 Objective of Thesis

The in-cylinder NO_x reduction using EGR has been implemented and used in diesel-fuelled vehicles. The alcohol fuels such as ethanol and n-butanol can potentially be used in diesel engines with some modifications in the fuel delivery system. The previous studies have shown that the use of alcohol fuels can reduce NO_x and PM emissions simultaneously [18,26,27]. However, to meet the NO_x emission regulations, an after-treatment system such as an LNT is required for further reduction in engine-out NO_x emissions. The use of ethanol and n-butanol as reductants for an LNT regeneration has not been explored much in the past.

The primary objective of this research is to investigate the NO_x reduction during the LNT regeneration using ethanol and n-butanol as reductants. The LNT regeneration performances with ethanol and n-butanol are compared with diesel that is conventionally used as a reductant on diesel vehicles. The LNT regeneration performance is compared in terms of NO_x conversion and by-product formation (e.g. NH_3 & N_2O) for different reductant types. The secondary objective of this work is to investigate the effect of the combined LNT-SCR after-treatment system on the overall NO_x reduction. This study is divided into 2 sections. The first section includes the engine test results conducted to demonstrate the exhaust conditions that are suitable for long breathing LNT operation. The second section comprises of the results and discussions related to the LNT regeneration and the combined LNT-SCR after-treatment system tests. The premise of the present study is to demonstrate strategies for ultra-low NO_x emissions using in-cylinder techniques, and after-treatment systems.

Initially, engine test results for diesel, n-butanol, and ethanol-diesel combustion are discussed to demonstrate low NO_x and PM emissions simultaneously. The engine exhaust conditions suitable for long breathing LNT operations are determined. In accordance, experimental investigations are performed using an LNT catalyst on an offline after-treatment system test bench under the simulated engine exhaust like conditions. The reductant is used only during regeneration for the NO_x reduction. Therefore, the adsorption period is not investigated in detail for this study, and adsorption is decoupled from the LNT regeneration period. Comprehensive analyses of different nitrogen-based species (e.g. NH_3 and N_2O) and HC species are performed based on the FTIR measurements. The combined LNT-SCR tests are performed to analyze the effect on the overall NO_x reduction by utilizing the NH_3 formed during the LNT regeneration on downstream SCR. The research methodology for this study is shown in Figure 1-11.
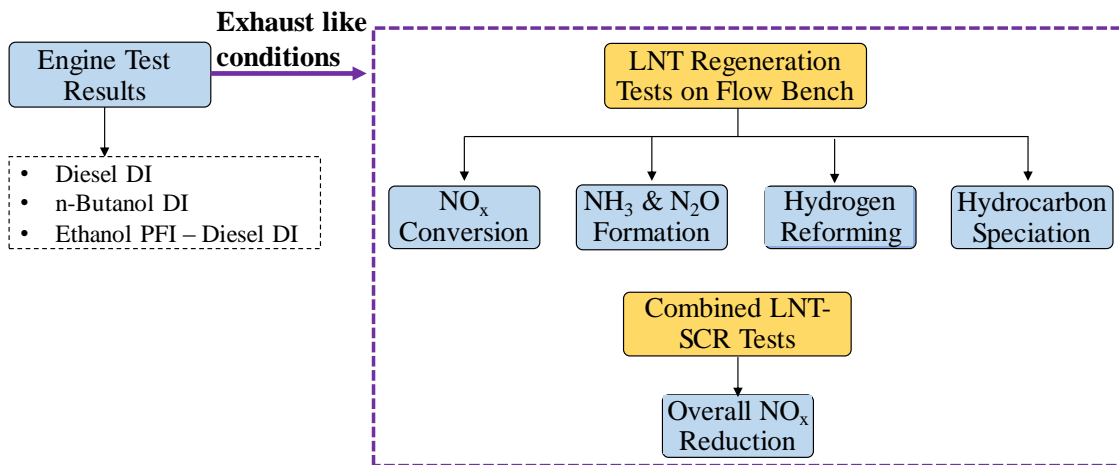
Figure 1-11: Research methodology

1.5 Structure of Thesis

Chapter 1 includes an overview of diesel engine emissions, emission legislations, in-cylinder emission reduction pathways, and exhaust after-treatment systems.

17

Chapter 2 contains the literature review related to adsorption and regeneration operation of LNT, H_2 reforming, and combined LNT-SCR after-treatment systems. The product formation due to the reduction of stored NO_x during the LNT regeneration has been elucidated in this chapter.

Chapter 3 provides a detailed description of the experimental setup used in this research work. Details and schematics related to engine test setup are explained with the emission analyzers in the initial part followed by the after-treatment flow bench test setup for the DOC-LNT and DOC-LNT-SCR configurations.

Chapter 4 pertains to the engine test results with diesel direct injection (DI), n-butanol DI and ethanol port fuel injection (PFI) – diesel DI performed on a single cylinder research engine.

Chapter 5 comprises of explanations and discussions about the test results related to the performance of LNT regeneration using diesel, ethanol, and n-butanol as reductants. The formation pathway of NH_3 and N_2O due to the reduction of stored NO_x, along with the hydrocarbon speciation and H_2 reforming during LNT regeneration is discussed. The H_2 reforming experimental results using ethanol and n-butanol as reductants are provided to explain the NH_3 formation and NO_x reduction.

Chapter 6 recapitulates the conclusions along with limitations and future recommendations for the present work.

CHAPTER 2: LITERATURE REVIEW

Although, the lean NO_x trap (LNT) has been used for NO_x reduction in diesel-fuelled vehicles for more than a decade, urea-based selective catalytic reduction (SCR) technology has gained popularity over the LNT after-treatment system. Currently, in order to meet more stringent regulations, the LNT combined with the SCR technology is also implemented [42]. In this chapter, literature reviews for the LNT operation during adsorption and regeneration period are performed with a focus on the different operating parameters that affect the NO_x conversion during regeneration. Studies of nitrogen-based species such as NH_3 and N_2O with the NO_x conversion during regeneration are also essential as they are undesired by-products. However, the NH_3 released during the LNT regeneration can be utilized on the SCR for further NO_x reduction. Therefore, at the end of this chapter, a review of the combined LNT-SCR after-treatment system is produced.

2.1 Lean NO_x Trap After-treatment System

Lean burn gasoline and diesel engines often have lower fuel consumption compared to stoichiometric SI engines [1,2]. However, a major problem in lean burn is the reduction of NO_x from engine exhaust, because three-way catalytic (TWC) convertor cannot reduce NO_x effectively under excess O_2 conditions. As a solution, the LNT technology can be used for NO_x reduction under lean burn (excess O_2) engine operations. An overview of NO_x reduction using an LNT catalyst is explained as follows.

2.1.1 Lean NO_x Trap Operation

The LNT operates under the periodic adsorption (lean) and regeneration (rich) cycles. During the lean period (storage period), the NO_x is continuously stored on the storage sites,

until the storage sites are saturated - beyond which NO_x cannot be stored. A typical LNT catalyst contains precious group metals (e.g. Pt and Pd), which helps in the oxidation of NO to NO_2, and an alkaline earth metal or basic phase (Barium oxide/carbonate) for providing a storage capacity as nitrite (NO_2^-) or nitrate (NO_3^{1-}) [46-49]. The two reactions during the NO_x adsorption are supported on the alumina (Al_2O_3) substrate. The alumina is used because it provides higher surface area and thermal stability. After NO_x adsorption, the LNT needs to be regenerated to reduce the stored NO_x with the help of a reductant. An LNT catalyst periodically undergoes rich conditions to regenerate the storage sites for a few seconds, during this period the stored NO_x is reduced to N_2 and other species [46-49]. Toyota introduced the NO_x storage and reduction (NSR) technique in the mid-1990s for vehicle emission control [39,40]. Since then researchers have investigated the LNT catalysts on heated reactors, engine dynamometers and real world driving vehicles. The chemical reaction models for the NO_x storage and reduction on an LNT catalyst using H_2, CO and propene (C_3H_6) as the synthetic gases has also been reported [47-50].

During the NO_x adsorption period, the NO_x storage efficiency is affected by the exhaust temperature, gas concentration, residence time and catalyst properties. The NO_x storage on the catalyst surface occurs via two chemical routes; nitrite route and nitrate route [46-50]. The NO to NO_2 oxidation is important in NO_x storage processes because NO_2 is more effective for the BaO loading, which is evident in literatures [42,46]. Henceforth, at low temperatures, the NO_x storage efficiency is low as a result of limited NO to NO_2 conversion [46].

The NO oxidation is also affected by the Pt dispersion and Pt particle size present on the catalyst [51,52]. Bhatia *et al.* have reported that the NO conversion reaches a maximum of

60% conversion around 350°C. The complete oxidation of NO to NO_2 over the Pt sites is constrained by thermodynamic NO/NO_2 equilibrium, kinetics, and mass transfer [51]. Lindholm *et al.* investigated the effect of H_2O and CO_2 on the NO_x storage efficiency of a Pt based LNT catalyst [53]. It was reported that the storage efficiency is higher in the absence of H_2O and CO_2. The CO_2 effect was significant than H_2O on the NO_x storage. Researchers have also investigated the effect of NO_x feed on the storage efficiency during adsorption period [44,45]. The NO_x storage efficiency decreased with the increase in NO feed at a 350°C LNT temperature [45].

The LNT regeneration period for the NO_x reduction is required to vacate the storage sites (BaO), occupied by NO_x. After a certain amount of the NO_x is stored, the LNT regeneration period is initiated with the help of a reductant. During regeneration, the catalyst temperature increases, and the O_2 concentration decreases that decreases the stability of Barium nitrites, and Barium nitrates, initiating their breakdown [46]. The stored NO_x is reduced to mainly N_2, and by-products in certain fractions during regeneration. A small amount of unconverted NO_x is also released instantaneously at the start of regeneration [46-49]. Different types of reductants such as H_2, CO, and hydrocarbons (HC) have been investigated in the past for the LNT regeneration [40,46-49]. It has been reported that H_2 is more efficient in NO_x reduction during the LNT regeneration [40]. Takahashi *et al.* investigated the performance of NO_x storage and reduction catalyst under low temperature and found that reduction efficiencies with the reductant type decrease in the order of $H_2 > CO > C_3H_6$ [40]. It was found that the NO_x storage sites were not regenerated completely when excess CO and C_3H_6 were used as reductants. However, the NO_x storage sites were completely regenerated when adequate H_2 was used as a reductant.

Maurer *et al.* recently investigated the effect of different space velocities, catalyst temperature and regeneration duration on the NO_x reduction efficiency and secondary emissions on a synthetic gas test bench [54]. During the lean period, 240 ppm NO_x, 6% CO_2, 6% H_2O, and 11% O_2 were supplied and for the rich period 1900 ppm C_3 C_3H_6, 2.7% CO, and 0.9% H_2 as a reductant with CO_2, O_2, H_2O were used. The variation in temperature showed that the LNT regeneration is most efficient between 300 to 400°C. An optimum temperature window for the NO_x storage was 300 - 350°C, and regeneration was very efficient at 350°C with low secondary emissions. The shorter regeneration period can be achieved with higher hourly space velocity (HSV). The CO & HC emissions decreased with the decrease in the regeneration duration without decreasing the LNT regeneration performance.

2.1.2 Product Formation during LNT Regeneration

The NH_3 and N_2O are two main nitrogen-based products formed during the LNT regeneration. The formation of both NH_3 and N_2O as a by-product is not desirable. The spatial profile of the stored NO_x along the catalyst length is schematically depicted in Figure 2-1. However, the NH_3 can be utilized on a SCR convertor downstream of an LNT catalyst for further NO_x reduction. The N_2O is a potential greenhouse gas (GHG), and formation is highly undesired. Researchers have reported that the N_2O formation occurs during the transition from either lean to rich or rich to lean conditions [55,56]. The N_2O formation occurs at the initial part on the regeneration sites on the LNT catalyst because of inadequate NO_x reduction over the PGM sites. Although, the N_2O is formed during rich to lean transition because of the reaction between the remaining adsorbed NO_x with the reductants.
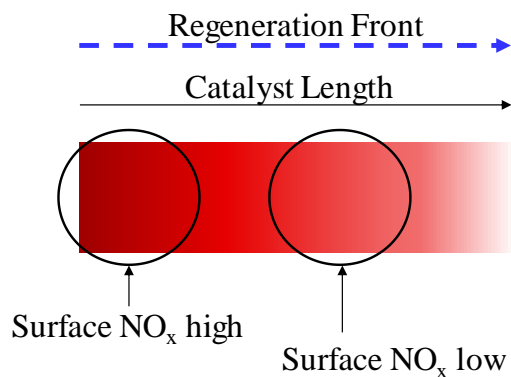
Figure 2-1: NO_x storage gradient on catalyst, adapted from [56]

Kubiak *et al.* reported the mechanistic aspects related to the formation of N_2O over the Pt-BaO/Al_2O_3 and $Rh-BaO/Al_2O_3$ model of NSR [57]. The H_2 and NH_3 were used as reductants to examine the reactivity of both gas phase NO and stored nitrates. It was observed that the gas phase N_2O formation involved the coupling of undissociated NO molecules with N-containing species formed upon NO dissociation on the reduced PGM sites [55,56]. The complete dissociation of the gas-phase NO can prevent N_2O formation. The N_2O formation appeared significant at low temperatures (near 150°C), while N_2O formation dropped at high temperatures (above 200°C). Since the reductant reduces the PGM sites effectiveness at a higher temperature, which leads to the complete dissociation of NO.

The NH_3 is formed by direct reaction of the NO_x and the available H_2 during the LNT regeneration. Castoldi *et al.* and Artioli *et al.* reported the reaction pathways given in Equation 2.1 and 2.2 for the NH_3 formation over the $Pt-Ba/Al_2O_3$ LNT catalyst [58,59]. Researchers found that initially, the reaction for NO_x reduction is selective towards N_2, but NH_3 is an intermediate product [58].

$$Ba(NO_3)_2 + 8H_2 \longrightarrow 2NH_3 + Ba(OH)_2 + 4H_2O \qquad \text{(Equation 2.1)}$$

$$Ba(NO_3)_2 + 8H_2 + CO_2 \rightarrow 2NH_3 + BaCO_3 + 5H_2O \qquad \text{(Equation 2.2)}$$
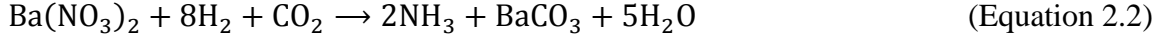
Many researchers have explored the effect of Pt and Ba concentrations on the NH_3 formation during regeneration [50-53, 60, 61]. Lindholm *et al*. investigated the impact of the catalyst preparation procedure on the performance of the LNT [60]. Two catalysts were prepared for experiments, one with Pt impregnated on Al/Ba and the other with Ba impregnated on Al/Pt. The experimental results showed an effect of preparation procedure on the NO_x storage and reduction LNT operation with N_2O and NH_3 formations. The NO_x storage capacity was higher for the catalyst with Ba impregnated on Al/Pt compared to the catalyst with Pt impregnated on Al/Ba at 400°C. The NO_x conversion was better with Al/Pt/Ba catalysts compared to Al/Ba/Pt catalyst due to well dispersed Ba for Al/Pt/Ba catalyst which leads to better contact between Ba and Pt. Castoldi *et al.* reported that NH_3 formation increased with the increase in Ba concentration on the catalyst, which also resulted in the slow release of H_2 during regeneration [61]. Literature data for the NH_3 formation during the LNT regeneration is summarized in Table 2.1.

Table 2.1 Literature data for NH_3 formation and H_2 consumption during regeneration

Author's	Castoldi *et al*. [58]	Artioli *et al*. [59]	Lindholm *et al*. [53]
Catalyst	Pt-Ba/Al$_2$O$_3$	Pt-Ba/Al$_2$O$_3$	Pt-Ba/Al$_2$O$_3$
Catalyst Temp. (°C)	350	350	400
NO inlet (ppm)	300	1000	300
NH$_3$ slip (ppm)	150-400	500	300
H$_2$ intake (ppm)	2000	4000	2000
H$_2$ slip (ppm)	600-1500	1000	80

2.2 On-board Hydrogen Reforming

On-board reforming of hydrocarbon fuels to produce hydrogen can be beneficial for the LNT catalyst operation. The presence of H_2 during the LNT regeneration improves the NO_x conversion and increases the NH_3 formation [40,45]. The catalytic H_2 reforming can occur through the following processes; steam reforming (SR) (Equation 2.3), partial oxidation (2.4), auto-thermal reforming (ATR) (Equation 2.5), and a combination of two or more methods [62].

$$C_xH_y + xH_2O \leftrightarrow \left(x + \frac{y}{2}\right)H_2 + xCO \qquad \text{(Equation 2.3)}$$

$$C_xH_y + \frac{x}{2}O_2 \leftrightarrow \frac{y}{2}H_2 + xCO \qquad \text{(Equation 2.4)}$$

$$C_xH_y + \frac{x}{2}O_2 + xH_2O \leftrightarrow \left(x + \frac{y}{2}\right)H_2 + xCO_2 \qquad \text{(Equation 2.5)}$$
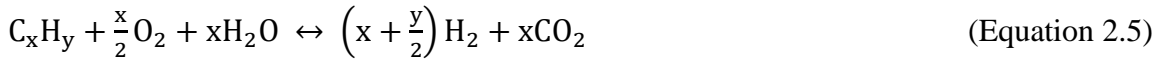
The steam reforming process yields a higher quantity of H_2 when the steam reacts with a hydrocarbon fuel. However, this requires a substantial amount of heating since it is an endothermic reaction [62]. The main products from the steam reforming of alcohol fuels are H_2, CO, CH_4, CO_2 and minor species (e.g. aldehydes, ethylene, coke) [63]. The alcohols are reactive molecules, which decompose over the catalyst surfaces (or in gas phase) much faster than hydrocarbons [63, 64].

The catalytic partial oxidation involves the incomplete combustion reaction of air-fuel mixture, thus producing the least amount of H_2 compared to other reforming processes [62]. The auto-thermal reforming involves both partial oxidation and steam reforming to result in thermodynamically neutral reaction [62]. Even though the H_2 yield is lower than steam reforming, thermodynamically neutral reactions are beneficial. Gutierrez *et al*.

investigated the auto-thermal reforming of ethanol over Rh and Pt mono and bimetallic catalyst [65]. It was reported that the complete conversion of ethanol occurred above 700°C when Rh catalyst is used.

The H_2 can also be produced via water-gas shift reaction on the catalyst (Equation 2.6). To increase the H_2 yield, combination of SR, ATR and water-gas shift reaction is often proposed by researchers [63].

$$CO + H_2O \rightarrow CO_2 + H_2 \hspace{4cm} \text{(Equation 2.6)}$$

2.4 Combined LNT and SCR After-treatment Systems

Studies have shown that the presence of a SCR convertor downstream of an LNT catalyst can improve the overall NO_x conversion [66-69]. In combined LNT and passive SCR systems, the fuel is solely required for the LNT regeneration. The SCR utilizes the NH_3 formed during the LNT regeneration. This entails that SCR can operate without urea injection system in combined configuration. Wang *et al*. studied the coupled LNT-SCR system for NO_x reduction consisting of Pt/Rh LNT catalyst and Cu-zeolite SCR [66]. The LNT catalyst temperature was maintained 200°C under the feed of 5% CO_2, 5% H_2O, 8% O_2, 300 ppm NO during lean period. During rich conditions of 5 seconds, the feed gas comprised of 300 ppm NO, 3333 ppm C_3H_6 or 5000 ppm C_2H_4, 0% or 1% O_2 (as indicated), 5% CO_2, 5% H_2O, and N_2 as balance. The test data was gathered at 25°C temperature interval up to 450°C. It was demonstrated that the Cu-SCR was better for the NO_x reduction using both alkenes and NH_3.

Bradley Gough *et al.* investigated the performance of the LNT catalyst with ethanol as a reductant [68]. This research was conducted for specific markets in which ethanol

infrastructure is developed (e.g. Brazil). The LNT catalyst was developed for >95% NO_x reduction using ethanol fuel reductant. The SCR and DOC were arranged in series to avoid the slip of the secondary emission produced during the regeneration. The after-treatment system was tested for different emission test cycles on 7.2 L and 13 L diesel engines. The results showed that the increase in the C/N ratio (i.e. ethanol to NO_x ratio) enhanced the NO_x conversion, however, led to the increased ethanol consumption and secondary emissions.

In summary, the LNT technology has proven to be very useful in NO_x reduction under lean burn engine operations. The researchers have explored the effect of different parameters such as temperature, gas composition, reductant types and catalyst properties on NO_x adsorption and reduction. The formation of by-products (e.g. NH_3 and N_2O) because of NO_x conversion in an LNT catalyst has also been studied in the past. A significant research has been conducted on the LNT regeneration operation using different reductants. However, there is not much literature available on the LNT regeneration performance using alcohol fuels (e.g. n-butanol and ethanol) under the engine exhaust like conditions. Therefore, in this research, investigations are performed to provide a comparison of NO_x conversion and species formation during the LNT regeneration using ethanol, n-butanol, and diesel as reductants. The potential of combined LNT-SCR (without urea) in NO_x reduction has also been explored in this work using n-butanol as a reductant for the LNT regeneration.

CHAPTER 3: EXPERIMENTAL SETUP

In this chapter, research tools used for the experiments are explained with help of schematics. The measurement instruments used for the engine and after-treatment flow bench tests are described. A heated offline after-treatment system test bench setup used for the LNT regeneration and the combined LNT-SCR tests is described in the later part of this chapter.

3.1 Engine Test Setup

The following engine tests are conducted on a 2.0 L Ford Duratorq diesel engine at the Clean Combustion Engine Lab (CCEL) at the University of Windsor. This 4-cylinder engine is converted into a single cylinder research engine with the other 3 cylinders kept at motoring [18]. The engine is coupled to a Schenck WS230 eddy-current dynamometer. The engine specifications are given in Table 3.1.

Table 3.1 Test engine specifications

Research Engine	Ford Duratorq
Engine Type	4-Cylinder (4-stroke)
Displacement (cm^3)	1998
Bore (mm)* Stroke (mm)	86 * 86
Compression ratio	18.2:1
Direct injection system	Common rail (max. 1600 bar)

The fuel injectors are actuated using the injector power drivers (iPOD), and an in-house developed LabVIEW program paired with National Instruments (NI) Real-Time (RT) and Field Programable Gate Array (FPGA) hardware. The engine speed is measured with a Gurley Precision Instruments 9125S optical encoder [70]. The in-cylinder pressure is

measured by a piezoelectric pressure transducer (AVL GU-13P) coupled to a Kistler Type5010 B charge amplifier. The pressure data is recorded at resolution of 0.1°CA, while 200 consecutive cycles are recorded for each test data point. The coolant temperature is maintained at 80°C using an external conditioning unit during the tests. Intake air is supplied through an oil-free dry air compressor, paired with an installed pressure regulator to control the mass flow rate. The intake and exhaust surge tanks are installed to provide steady intake and exhaust conditions. In turn, this decreases the cyclic pulsations generated by the valve opening and closing, thus reducing measurement error. Intake and exhaust gas compositions are determined through the emission analyzers. All the test data (e.g. emissions, pressure and temperature readings, fuel injection timing and duration) is synchronized through local area network, and shared variables in LabVIEW program.
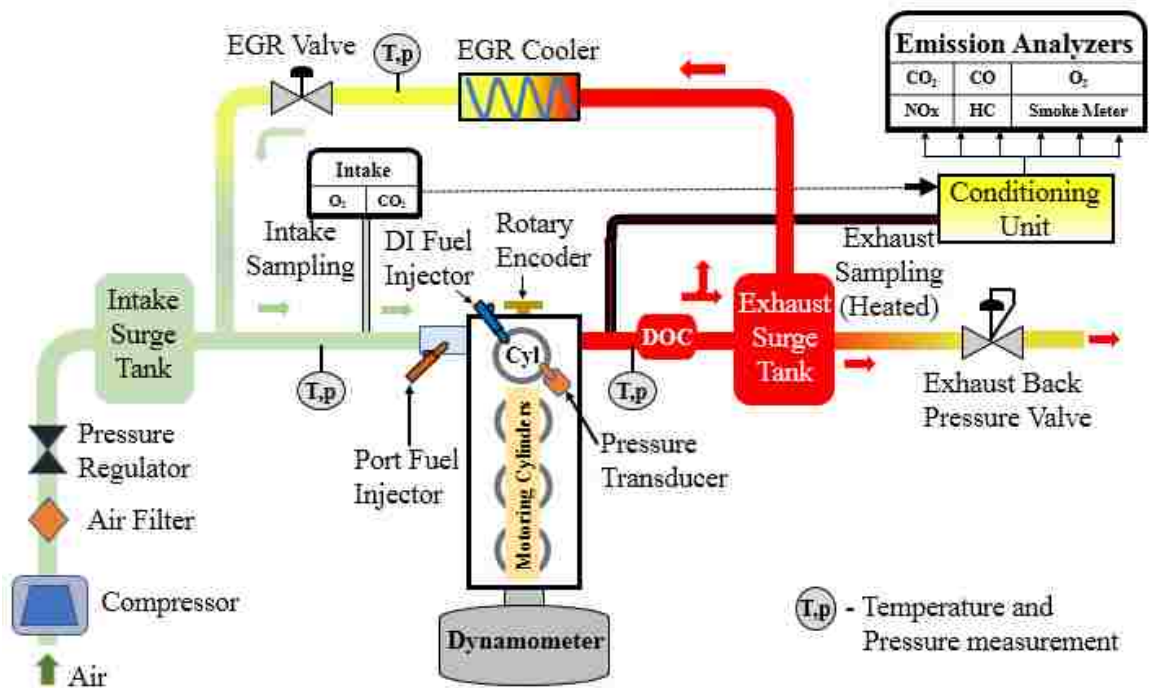
Figure 3-1: Engine test setup schematic

The fuels used for the engine tests include diesel, ethanol, and n-butanol. These fuels are also used as reducing agents (reductants) for the LNT regeneration tests. The high pressure direct injection (DI) is used for diesel and n-butanol delivery, whereas the port fuel injection (PFI) is used for the ethanol injection during the engine tests. The properties of the reducing agents for LNT regeneration used in this study are given in Table 3.2.

Table 3.2 Fuel properties [71-74]

Fuel Properties	Diesel	n-Butanol	Ethanol
Fuel Formula	$C_1H_{1.85}$	$C_4H_{10}O$	C_2H_6O
Lower Heating Value (MJ/kg)	43.5	33.1	26.8
Carbon Content (% mass)	86.8	64.8	52.1
Hydrogen Content (% mass)	13.2	13.6	13.1
Oxygen Content (% mass)	0	21.6	34.8
Density @ 15°C, (kg/m^3)	858	813	788
Viscosity @ 40°C, (cSt)	2.7	3.6	1.5
Boiling Temperature @ 1 bar, (°C)	Variable	117.5	78.3
Cetane Number	46.5	25	10
Octane Number	25	87	110
Lubricity (μm) from HFRR*	315 [72]	591 [72]	1057 [72]
Purity	-	>997 [73]	>99.5 [74]

* HFRR: High-Frequency Reciprocating Rig

3.2 Emission Analyzers

During the engine tests, intake and exhaust gases are directly sampled by using a dual-bank gas analyzer. The sampled gases firstly pass through a conditioning unit that consist of a chiller unit, a heated pump, and numerous filters to remove PM and water concentration. The intake and exhaust CO_2, alongside exhaust CO, are measured using the California

Analytical Instruments (CAI) non-dispersive infrared analyzers. The CAI chemiluminescence and flame ionization detectors are used to measure the NO_x and THC respectively during the engine and after-treatment flow bench experiments. All the CAI analyzers are calibrated before each test. For full scale operating range of CAI analyzers, the noise, zero drift, repeatability, and linear uncertainties are each below 1%. An AVL smoke meter (Model 415S) is used for smoke measurement during the engine tests. The specifications of different emission measurement devices used in the engine and the after-treatment flow bench tests are tabulated in Table 3.3. An MKS 2030 DS Fourier transform infrared (FTIR) spectrometer is used to measure the NH_3, N_2O, and hydrocarbon species during the LNT regeneration experiments [75].

Table 3.3 Emission analyzers specifications

Analyzer type	Measured Emissions	Model	Range used	Resolution	Noise/Zero Span Drift
Paramagnetic detector	O_2 (%)	CAI 602P	0-25%	0.025%	<1%
Heated Flame Ionization Detector	THC (ppm C1)	CAI 300 HFID	0-3000 ppm	0.01 ppm	<1%
Heated Chemiluminescence Detector	NO and NO_2 (ppm)	CAI 600 HCLD	0-3000 ppm	0.01 ppm	<1%
Non-Dispersive Infrared	CO (ppm) and CO_2 (%)	CAI 200/300 NDIR	CO: 0-1% CO_2: 0-20%	CO – 0.001% CO_2 – 0.02%	<1%

3.3 After-treatment Flow Bench Setup

The after-treatment system tests are conducted on a separate flow bench from engine test setup. The engine exhaust like conditions are simulated on the flow bench for the experiments. An LNT catalyst is the primary after-treatment system studied in this

research. The flow bench is developed at the CCEL for after-treatment system research [44,45]. The schematic of the flow bench is shown in Figure 3-2.
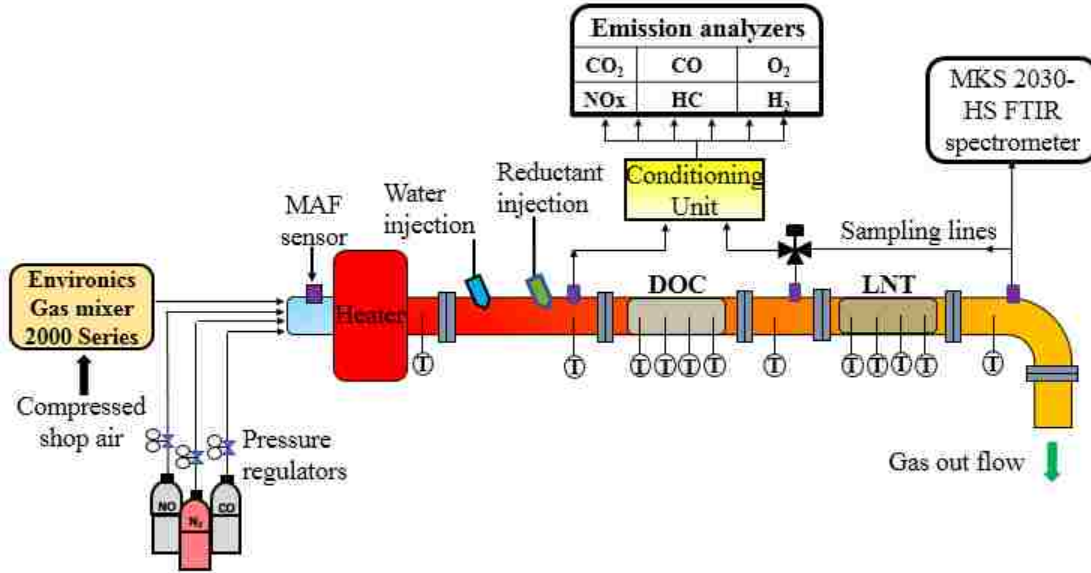
Figure 3-2: After-treatment flow bench test setup schematic

Commercially available catalysts (e.g. DOC, LNT, and SCR) are used in this research, without modifications to their respective catalytic properties. The volume of the catalysts used is 0.234 litres. The LNT catalyst used for the experiments is $Pt/Ba-Al_2O_3$. The copper-exchanged zeolite SCR is used for investigation. A fiber mat for thermal insulation is used to reduce the heat loss, is provided around the 2" diameter steel pipe sections in which catalysts are kept.

Praxair compressed gas cylinders are used to supply NO, CO, and N_2 at a required concentration to the flow bench. The pressure regulators are used to control flow from the NO, CO and N_2 gas cylinders. Compressed air at 4 bar is supplied to the Environics Series 2000 Multi-Component Gas Mixer. The Gas Mixer is used to control air flow rate. The inflow O_2 concentration on the bench is achieved by regulating the flow of air through Gas

Mixer and balance N_2 gas from the cylinder. "Tera Term" program is used to control the Gas Mixer remotely during tests. A mass air flow (MAF) sensor from Bosch (model - 0281002619) is installed upstream of the heater. An SCXI-1302 module is used to acquire the measurement from a MAF sensor. The PM in the exhaust can be filtered using a diesel particulate filter. Therefore, PM is not considered in this investigation. A Leister LE 10000s Electric Hot Air Tool heater, rated up to 650°C maximum temperature is used to maintain the required temperature during tests. The Omega "K" type thermocouples are used, alongside an NI SCXI-1303 terminal block and an SCXI-1102 thermocouple module, for temperature data measurement and acquisition.

The reductant and water injection are done using low-pressure injectors that are designed originally for gasoline PFI. For the experiments, the injection pressure is maintained constant at 2.5 bar gauge. Both are injected into the heated feed gas directly. A water cooling jacket is provided around both the injectors to avoid damage at high temperatures. Deionized water is used for the water injection. The quantity of reductant and water required during the LNT regeneration is achieved by varying the parameters such as length, frequency, and duty cycle of the pulse width modulation (PWM) signal. Initially, both the water and reductant injectors are calibrated. The duty cycle and frequency combinations are identified before the experiments to inject the required quantity of water and reductant. The user defined injection command is sent from personal computer (PC) to an NI PXI-8110 real-time computer. An NI PXI-7853R FPGA module, which is connected to the RT computer generates the desired PWM signal. The PWM signal is then sent to an in-house built injector driver circuit. The parameters are controlled using an in-house developed NI LabVIEW program paired with RT and FPGA hardware.

The gas sampling is implemented at upstream of the DOC and downstream of the LNT catalyst during the LNT regeneration experiments. The CAI analyzers mentioned earlier in this chapter are used to analyze gas composition upstream and downstream of the catalysts. The program developed using the LabVIEW software is used to monitor, record and synchronize all the test data. Apart from CAI emission analyzers, an MKS 2030-HS FTIR spectrometer is used to measure the concentration of the species such as NH_3, N_2O and hydrocarbons. A V&F Q7000 hydrogen analyzer is used to measure the H_2 that is formed during the LNT regeneration process [76].

For the combined LNT-SCR after-treatment system tests, the previous test setup is modified after the LNT catalyst, and a commercially available Cu-SCR is placed downstream of the LNT catalyst, as shown in Figure 3-3. To investigate the effect of SCR on overall NO_x abatement, gas sampling is implemented before and after the SCR. The average temperature achieved on the SCR during test is ~265°C with the average LNT temperature maintained at ~350°C during adsorption.
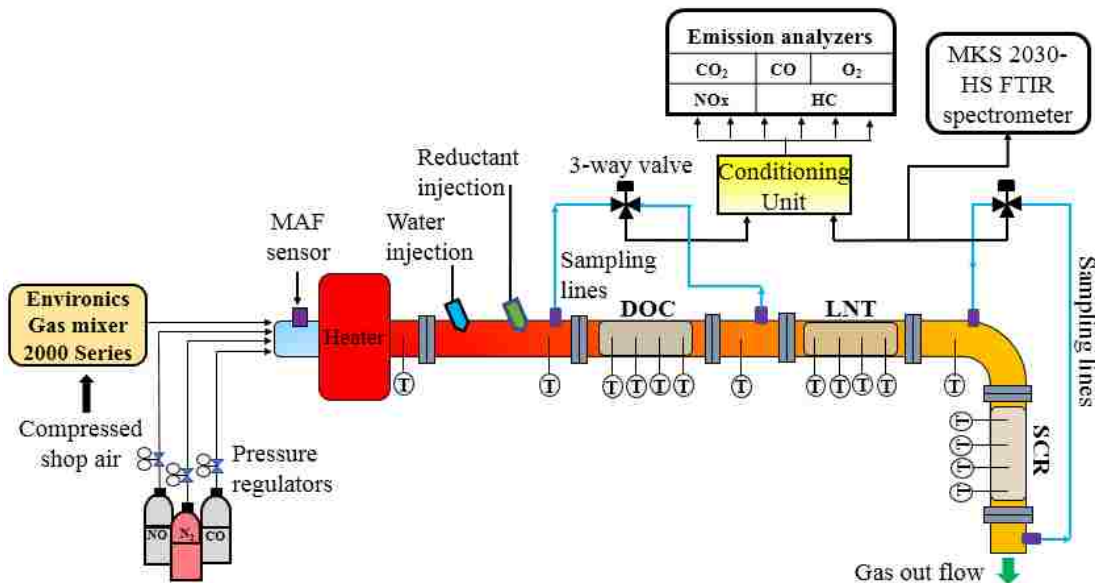
Figure 3-3: Test setup schematic for combined LNT-SCR tests

CHAPTER 4:   ENGINE TEST RESULTS

In this chapter, engine test results are discussed. The engine tests are conducted at the Clean Combustion Engine Laboratory at the University of Windsor. The engine tests are performed to determine the engine-out exhaust conditions suitable for long breathing LNT operations. As discussed earlier, NO_x reduction can be achieved by using in-cylinder approach such as EGR and alternative fuels. The engine tests with diesel, n-butanol, and ethanol are conducted with the application of EGR. All the tests are performed at the medium engine load (10 bar IMEP – Indicated Mean Effective Pressure). The engine test conditions are shown in Table 4.1. The emission regulations are enforced on a brake-specific basis. However, emission levels in this chapter are reported on an indicated basis, and thus a lower indicated emission level could be required to satisfy the regulations.

Table 4.1 Engine test conditions

Fuel	Diesel	n-Butanol	Ethanol – Diesel (60:40)
IMEP (bar)	~ 10	~ 10	~ 10
Speed	1500	1500	1500
Injection pressure, p_{inj} (Mpa)	120	90	120
Port Fuel p_{inj} (bar)	-	-	7
Intake pressure, p_{intake} (bar)	2	2	2
CA50 (°CA)	368	369	368
EGR Sweep (Intake O_2 %)	14.2-18.5%	14.5-18.5%	14.5-18.4%

4.1 Diesel DI Medium Load Engine Test

Firstly, diesel is used for the medium load engine tests. To maintain the medium load, the fuel injection duration and pressure are set to 610 μs and 1200 bar, respectively. The intake

boost pressure of 2 bar absolute is used. The fuel injection timing is varied between 354°CA to 358°CA to maintain the CA50 (50% mass fraction burned) around 368°CA. The effect of EGR on NO_x and PM at the medium engine load is shown in Figure 4-1. The well-known NO_x and soot trade-off is evident. A major decline in NO_x emission is observed from 750 ppm to 100 ppm, when the intake O_2 concentration changes from 18% to 15.5% as a result of EGR application. The PM levels are below 0.01 g/kW·hr at 16.33% intake O_2 concentration. However, the PM emissions are increased with a further increase in the EGR. The PM can be filtered in exhaust by using a diesel particulate filter (DPF). Generally, modern diesel vehicles are equipped with a DPF, known to have a filtration efficiency of more than 95%. Therefore, to meet the current PM emission limits of 0.013 g/kW·hr, the engine-out indicated PM emissions should be below 0.1 g/kW·hr, considering DPF filtration efficiency of 95%. For the long breathing LNT operations, NO_x and PM emission limits are ~100 ppm and ~0.1 g/kW·hr respectively [44]. Both NO_x and PM emissions should be below the limits simultaneously. It is clear from Figure 4-1 that at this engine test conditions, the PM emissions are higher than 0.1 g/kW·hr, when NO_x emissions are below 100 ppm.
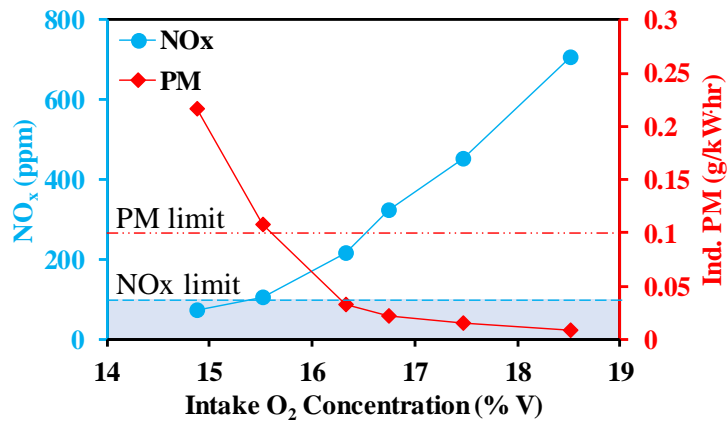
Figure 4-1: NO_x and PM emissions with diesel DI at medium load

36

The effect of EGR on CO and THC emissions is shown in Figure 4-2 at similar engine test conditions. The CO and THC emissions tends to increase with the application of EGR.
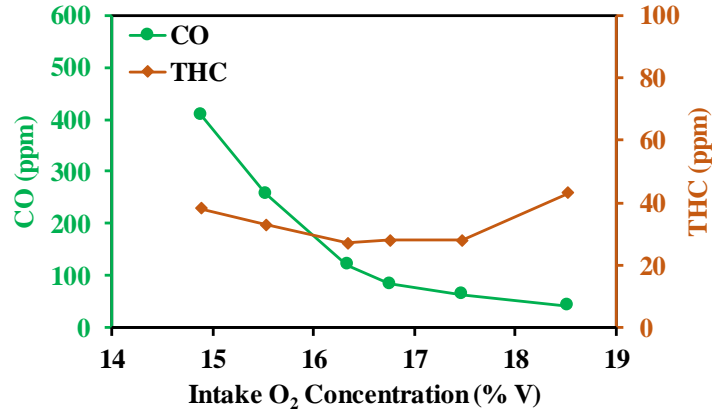
Figure 4-2: CO and THC emissions with diesel DI at medium load

4.2 n-Butanol DI Medium Load Engine Test

The second set of engine test are conducted using n-butanol with DI (direct injection). n-Butanol fuel can be used in a diesel engine with minimal modifications due to its high viscosity. However, it has been reported in the literatures that the peak pressure rise rates of using n-butanol at the medium and high engine load operations are challenging [18,71]. To accommodate for this challenge, a double injection strategy is employed in this set of engine tests. The first fuel injection timing is set to 343°CA, while second is set to 363°CA at the same injection pressure. Combustion phasing (CA50) is maintained at 369°CA throughout the EGR sweep. The effect of EGR on NO_x and PM at the medium engine load with the long breathing region is shown in Figure 4-3. The PM emission level are lower throughout the EGR sweep. Compared to the relevant test results with diesel DI in Figure 4-2, the NO_x and PM emissions of this set of engine tests are lower. The higher volatility and O_2 content in n-butanol helps in highly premixed and ultra clean combustion [18,70].

Moreover, NO_x and PM limits for long breathing conditions are achieved with n-butanol combustion. Under the same test conditions, the CO and THC emissions increase with the increasing EGR. The effect of EGR on CO and THC is shown in Figure 4-4.
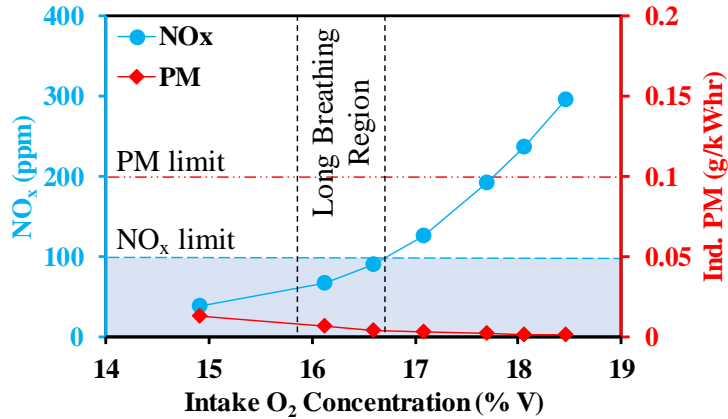
Figure 4-3: NO_x and PM emissions with n-butanol DI at medium load
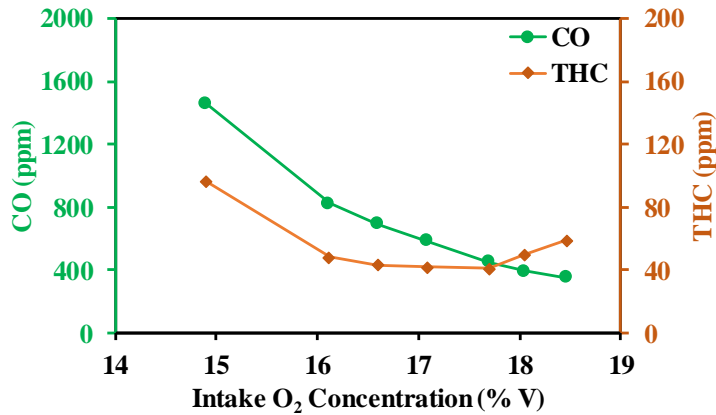
Figure 4-4: CO and THC emissions with n-butanol DI at medium load

4.3 Ethanol Diesel Dual-Fuel Medium Load Engine Test

The high-pressure direct injection (DI) of ethanol is challenging because of its high volatility and poor lubricity [71]. The ethanol is difficult to compression ignite compared

to the n-butanol because of lower reactivity. Therefore, the ethanol is delivered via port injection and the diesel via direct injection as a pilot fuel [18].

The engine tests are conducted at 10 bar IMEP with an ethanol to diesel energy ratio of 60:40 that showed the lowest NO_x emissions among the tested fuel ratios [77]. The ethanol as a port fuel is injected for 3400 μs at 7 bar injection pressure. The diesel is injected for fixed duration of 380 μs at varied injection timings in a range of 355°CA to 359°CA. The combustion phasing is maintained at 368°CA during the test. The effect of EGR on NO_x and PM emissions is shown in Figure 4-5. Conditions suitable for long breathing LNT operations are achieved with ethanol diesel dual-fuel combustion at the tested condition. The PM emissions are lower than 0.1 g/kW·hr throughout the EGR sweep.
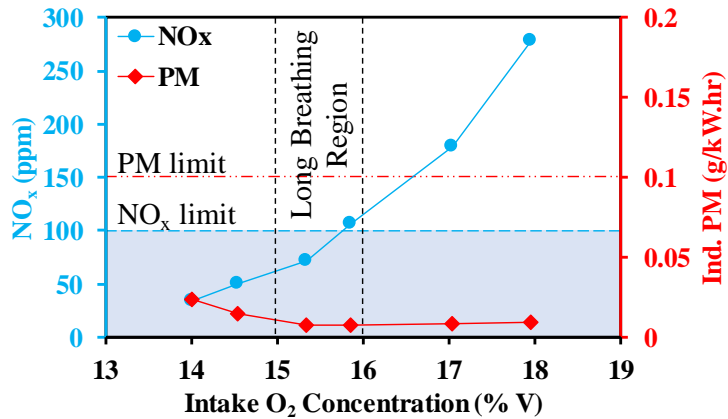
Figure 4-5: NO_x and PM emissions with ethanol-diesel at medium load

The effect of EGR on the CO and THC emissions is shown in Figure 4-6. The CO and THC emissions are significantly higher compared to the n-butanol DI and diesel DI combustion. This is attributed to the lower in-cylinder charge reactivity to effectively oxidize the CO and THC. Thus, the combustion efficiency is lower during ethanol diesel dual-fuel combustion [18,70].
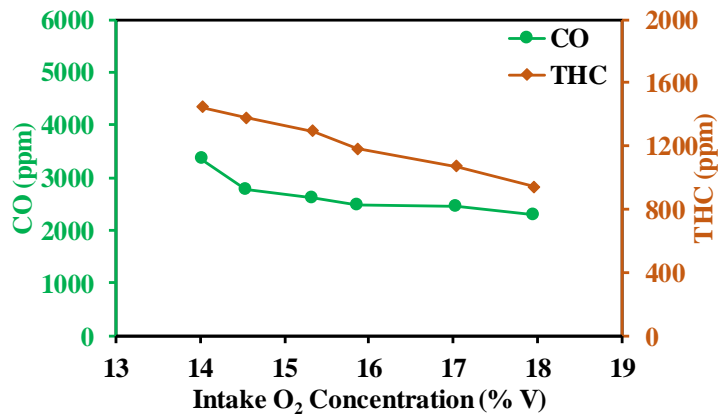
Figure 4-6: CO and THC emissions with ethanol-diesel at medium load

Summary

The NO_x formation is reduced with the application of EGR. However, the excessive application of the EGR leads to an increase in the PM emissions, and a reduction in the combustion efficiency. The NO_x and soot trade-offs are evident for all the engine tests. At moderate EGR (i.e. 15 to 17% intake O_2 concentration), the NO_x emissions could be limited to ~100 ppm for all cases. For n-butanol and ethanol-diesel cases, the indicated PM emissions are less than 0.05 g/kW.hr throughout tested EGR sweep. Thus, the ethanol-diesel and n-butanol combustion under the tested conditions satisfy the long breathing LNT operation requirements. Additionally, with the application of moderate EGR for ethanol-diesel and n-butanol cases, the NO_x and PM emissions are below 100 ppm and 0.1 g/kW.hr respectively. For the long breathing strategy, the engine exhaust O_2 volumetric concentration is measured to be around 8.5%. This volumetric concentration is used as a reference for the after-treatment system tests on an offline test bench.

CHAPTER 5: LNT REGENERATION INVESTIGATION

In this chapter, the LNT regeneration test results are discussed. To investigate the LNT performance with different reductants, the LNT regeneration tests are conducted. The engine exhaust like conditions are simulated on a flow bench for the LNT regeneration experiments. The experiments for the LNT regeneration period are performed using diesel, n-butanol, and ethanol as reductants at 3% and 8.5% inflow O_2 concentrations. The results for NO_x conversion and different products formation during regeneration are discussed. The results for HC species formed because of fuel reforming on the DOC and LNT catalyst are also presented. Furthermore, results for investigation of the combined LNT-SCR tests on the overall NO_x reduction have been explained at the end of this chapter.

5.1 LNT Test Methodology

The complete LNT operation cycle consists of adsorption, regeneration and purge period in this investigation. Firstly, the NO_x is adsorbed on the LNT catalyst for each test case. During adsorption period, the average LNT temperature is maintained at 350°C. The NO concentration of ~200 ppm with the balance air is supplied at the inlet of the flow bench. The inflow NO (i.e. NO feed) concentration of 200 ppm is chosen to reduce the adsorption time to ~5.5 mins to store cumulative NO_x of 0.21 g. The 0.21 g NO_x storage results in NO_x loading equivalent to 0.9 g/L of LNT catalyst. Based on the previous experiments on the flow bench, it has been observed that the NO_x loading of 0.9 g/L of LNT is the maximum suitable amount of NO_x until the regeneration would require a significantly higher amount of reductant [45]. The NO_x adsorption tests under the same conditions have shown that 100 ppm NO feed takes approximately 11 mins to store 0.21 g NO_x [41]. During the NO_x adsorption period, parameters such as inflow NO concentration, NO_x storage

quantity, hourly space velocity (HSV), and LNT temperature are kept the same for each test case.

The NO_x storage is calculated based on the difference between the inlet (sampling before DOC) and the outlet (sampling after LNT) NO_x concentration measured using emission analyzers. The NO feed is stopped when 0.21 g of NO_x storage is achieved on the LNT catalyst. The hourly space velocity (HSV) of 80,000 hr^{-1} is achieved during adsorption period. The NO_x slip (i.e. NO_x measured at the outlet of LNT) during the adsorption period is observed to be low (5-10 ppm) for each of the test case. The NO_x storage efficiency for all the test cases is around 97%. The storage efficiency is calculated based on Equation.5.1.

$$\text{Storage Efficiency} = \frac{m_{NOx\ intake} - m_{NOx\ slip\ during\ adsorption}}{m_{NOx\ intake}} \qquad \text{(Equation 5.1)}$$

The LNT regeneration period is initiated after the NO_x adsorption period is completed. The LNT regeneration tests are conducted under 3% and 8.5% inflow O_2 concentration. The inflow O_2 concentration of 8.5% is chosen based on engine exhaust like condition. The effect of oxygen is of interest, and 3% was the lowest achievable O_2 concentration for this flow bench setup. The 3% inflow O_2 is used to have a comparison with the previous experiments conducted at the CCEL [45]. During the LNT regeneration, HSV is achieved to be around 50,000 hr^{-1}. The LNT regeneration investigation is explained in section 5.2.

Each LNT regeneration test case is followed by a purge period for 1 min. A purge period is included to vacate the NO_x from storage sites on the LNT catalyst if it is not eliminated (i.e. reduced) during the LNT regeneration. The previous research has shown that if the reductant quantity is not sufficient to reduce the NO_x, a certain portion of the stored NO_x remains on the LNT, which can affect the next cycle of the LNT operation [45]. During the

purge period, 1% CO, 6% H_2O and balance N_2 are supplied without reductant injection. The LNT temperature during the purge period decreases because of water injection. The HSV during the purge period is kept similar to the regeneration period.

5.2 LNT Regeneration

The experiments for investigating the LNT regeneration are conducted at the steady state conditions. The LNT regeneration period is decoupled from the NO_x adsorption period during the experiments by not supplying NO_x during regeneration. The water and fuel injections are initiated once the inflow O_2 concentration and catalyst temperature are stable. The reductant injection period is kept 30 seconds during the LNT regeneration. The effect of reductant type on NO_x conversion, and by-product formation during the LNT regeneration are discussed in the following sections. The test conditions for LNT regeneration is given in Table 5.1.

Table 5.1 LNT regeneration test conditions

Reductant	LNT Temp (°C)	NO_x Stored (g)	Reductant Quantity (g)	O_2 (%)	H_2O (%)
Diesel	350	0.21	0.8	3 & 8.5	6
	350	0.21	1.7	3 & 8.5	6
	350	0.21	3.2	3 & 8.5	6
Ethanol	350	0.21	0.8	3 & 8.5	6
	350	0.21	1.7	3 & 8.5	6
	350	0.21	3.2	3 & 8.5	6
n-Butanol	350	0.21	0.8	3 & 8.5	6
	350	0.21	1.7	3 & 8.5	6
	350	0.21	3.2	3 & 8.5	6

5.2.1 NO_x Release during LNT Regeneration

The reduction of stored NO_x is initiated on the LNT catalyst with the reductant injection. After a few seconds of reductant injection, the NO_x slip from the LNT catalyst is observed

43

for all test cases. The slip of the instantaneous NO_x at 3% inflow O_2 concentration with 1.7 g of n-butanol as a reductant is illustrated as an example in Figures 5-1. When the reductant is injected, the catalyst temperature increases, and the O_2 concentration decreases. Consequently, this reduces the stability in barium nitrates, and barium nitrites. Thus, NO_x is released from the storage sites for reduction [41,46]. During the regeneration period, a certain fraction of the stored NO_x is released unconverted as shown in Figure 5-1.
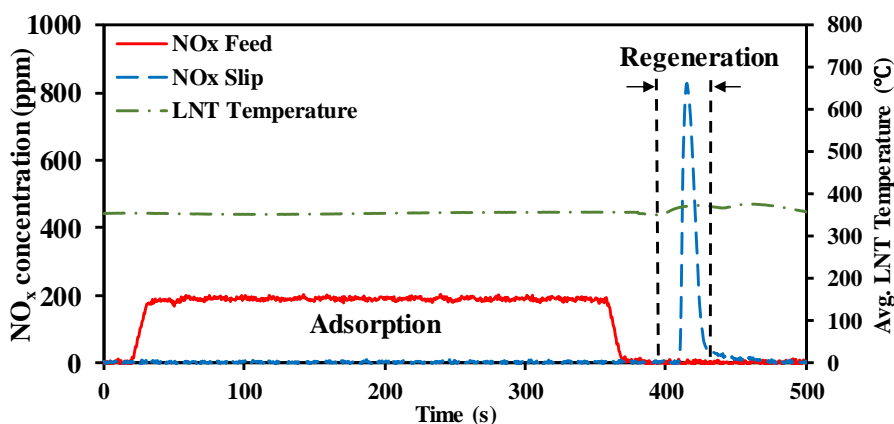
Figure 5-1: LNT regeneration at 3% inflow O_2 using 1.7 g n-butanol as a reductant

The peak value of NO_x slip during the LNT regeneration relative to the injected quantity of reductants is presented in Figures 5-2 and 5-3 for 3% and 8.5% inflow O_2 respectively. For all the reductants, the peak instantaneous NO_x slip increases with an increase in the injected quantity. The peak NO_x slip is higher with n-butanol than with ethanol at lower injected quantity. It has been suggested in literature that the presence of CO_2 significantly influences the reaction chemistry of the LNT catalyst during regeneration [78]. The NO_x conversion decreases in the presence of CO_2 during regeneration [78]. In the present investigation, CO_2 is not supplied to the flow bench. However, the CO_2 is generated in the flow bench as a result of the HC oxidation in the DOC and LNT catalyst. The CO_2 formation increases as the injected reductant quantity increases. Therefore, the increase in

the peak NO_x slip can be ascribed to the increase in CO_2 concentration and the increase in temperature during regeneration.
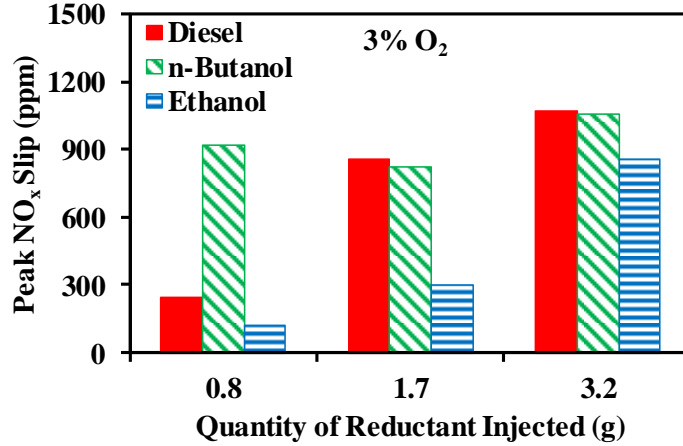
Figure 5-2: Peak NO_x slip during regeneration at 3% inflow O_2
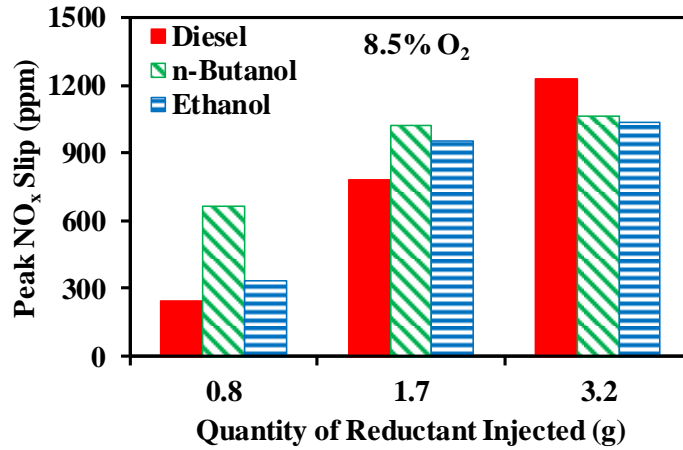
Figure 5-3: Peak NO_x slip during regeneration at 8.5% inflow O_2

The cumulative mass of NO_x slip per mass of stored NO_x relative to the reductant quantity under 3% and 8.5% inflow O_2 is illustrated in Figures 5-4 and 5-5 respectively. As the quantity of reductant injected increases, the percentage of NO_x slip for diesel and ethanol case also increases. However, a slight decrease in the percentage of NO_x slip is observed with the n-butanol case for both the inflow O_2 concentration. The NO_x slip during

45

regeneration is the highest with diesel and the lowest with ethanol as a reductant. This can be because of the lower volatility and H_2 production during regeneration using ethanol compared to ethanol and n-butanol as reductants. The presence of CO_2 inhibits the effective NO_x conversion process because the reverse water gas shift reaction leads to carbonyls formation on the PGM sites of the LNT catalyst [78]. Therefore, the mass of NO_x slip per unit mass of NO_x stored on the LNT increases with the increase in quantity for diesel and ethanol as reductants.
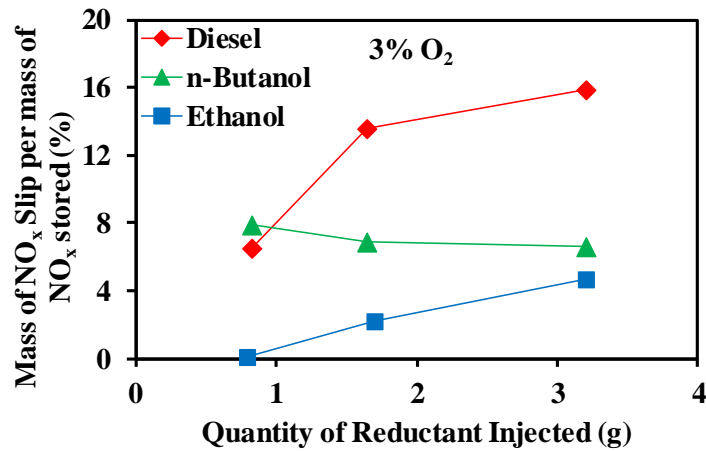
Figure 5-4: Mass of NO_x slip per mass of stored NO_x at 3% inflow O_2
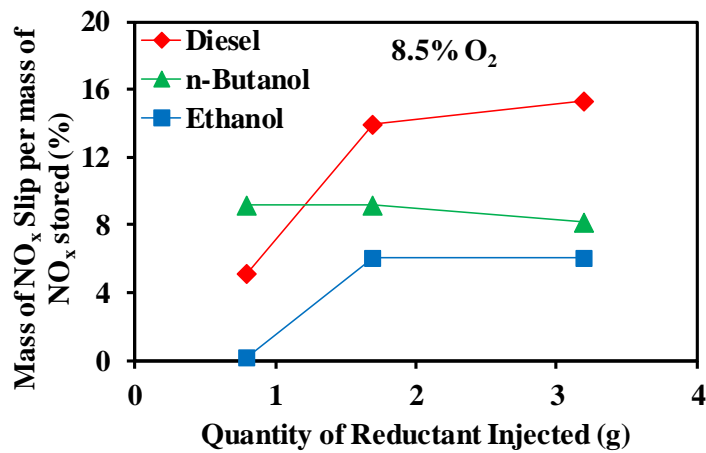
Figure 5-5: Mass of NO_x slip per mass of stored NO_x at 8.5% inflow O_2

The NO_x slip may also be compared with respect to the amount of reductant energy injected to reduce the NO_x. The amount of energy injected is calculated by multiplying the gravimetric energy density with the quantity of reductant. The trend for NO_x slip per mass of NO_x stored relative to the energy of reductant injected is demonstrated in Figure 5-6 for 8.5% inflow O_2 tests. The trend is similar in terms of quantity of reductant injected. However, it can be realized in Figure 5-6 that the lower amount of energy is injected for the LNT regeneration with ethanol and n-butanol than with diesel as a reductant.
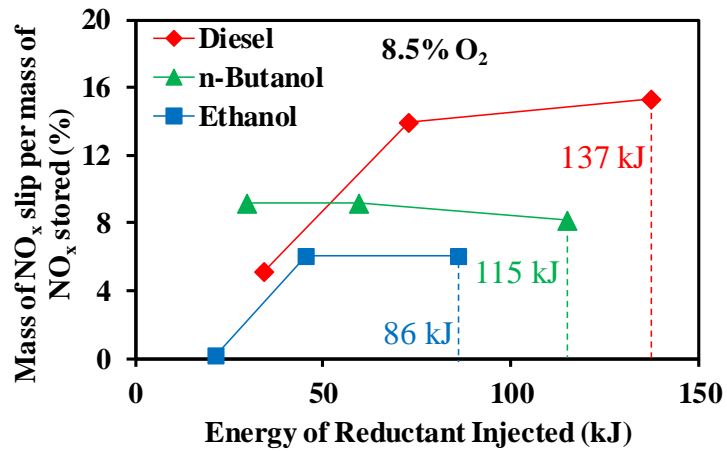
Figure 5-6: Mass of NO_x slip per mass of stored NO_x against reductant energy

The regeneration effectiveness is calculated using Equation 5.2 to evaluate the LNT regeneration [45]. The cumulative mass of the NO_x is used to calculate the regeneration effectiveness. The regeneration effectiveness is considered as 100% if no NO_x is released during the purge period. The purge period is crucial to determine the quantity of NO_x remained unconverted after the regeneration period. The LNT operation cycle consisting of adsorption, regeneration and purge period under the 8.5% inflow O_2 is illustrated in Figures 5-7 and 5-8. Theses figures serve as an example for n-butanol and diesel cases.

$$\text{Regeneration Effectiveness} = \frac{\text{NO}_x \text{ stored} - \text{NO}_x \text{ slip during purge}}{\text{NO}_x \text{ stored}} \quad \text{(Equation 5.2)}$$

The regeneration effectiveness is considered 100% for test cases with no NO_x slip during the purge period. During purge period, no NO_x release is observed for both n-butanol and ethanol as reductants at the two tested O_2 concentrations. Moreover, during the purge period for the highest quantity (i.e. 3.2 g) of injected diesel, there is no NO_x released. However, for 0.8 g and 1.7 g of injected diesel, there is a certain fraction of the stored NO_x that is released during the purge period. The release of this NO_x during the purge period leads to reduced regeneration effectiveness. The lower regeneration effectiveness with diesel as a reductant could be related to the insufficient quantity of diesel injected to reduce the stored NO_x. The WGS reaction and steam reforming on the DOC and LNT increases the total H_2 yield. The presence of higher H_2 could potentially contribute to higher regeneration effectiveness. The H_2 measurement is performed in this investigation during the LNT regeneration for further verification and discussed in section 5.3.
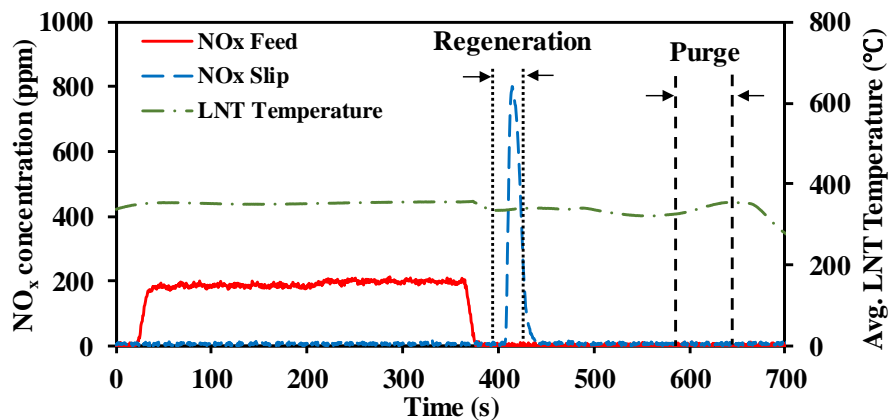
Figure 5-7: LNT regeneration with 1.7 g n-butanol followed by purge period
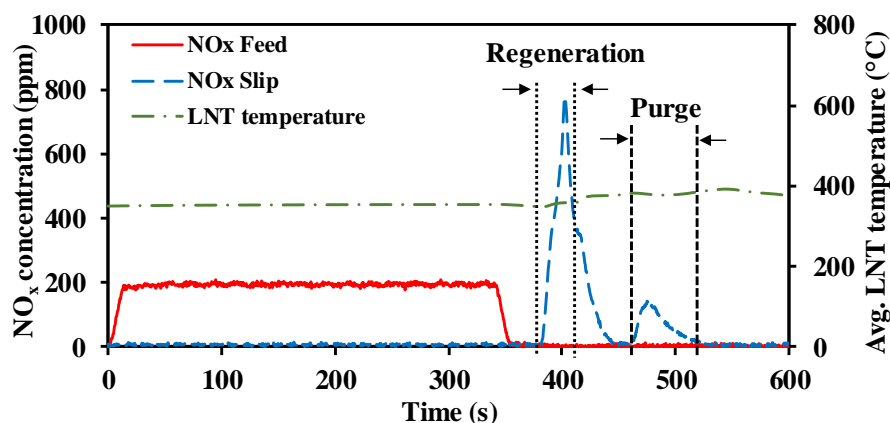
Figure 5-8: LNT regeneration with 1.7 g diesel followed by purge period

5.2.2 Product Selectivity during LNT Regeneration

The selectivity in a chemical reaction is entitled as the tendency of reactants to form a product over other products. During the LNT regeneration, higher conversion of the stored NO_x into N_2 is desirable. However, other by-products are also formed during the regeneration period. The product formation because of the NO_x conversion during the LNT regeneration is investigated in this research. The FTIR is used to measure the concentration of NH_3 and N_2O. In the same set of LNT regeneration tests (refer to Table 5.1), sampling for the FTIR measurement is performed after the LNT.

The cumulative molar quantities of NH_3 and N_2O formed during the LNT regeneration are analyzed in terms of product selectivity. The selectivity towards N_2O and NH_3 is calculated using Equations 5.3 and 5.4 respectively [45,79]. The cumulative molar N_2O and NH_3 are represented as $[N_2O]$ and $[NH_3]$ respectively. Both the stored and released molar NO_x quantities are represented as $[N]_{inflow}$ and $[NO_x]$ respectively in the given equations. Although, direct measurement of N_2 is not performed, an estimation is made for the N_2 selectivity considering that stored the NO_x is converted into N_2, NH_3, and N_2O during regeneration.

49

$$N_2O \text{ Selectivity} = \frac{2[N_2O]_{regeneration}}{[N]_{inflow}} \qquad \text{(Equation 5.3)}$$

$$NH_3 \text{ Selectivity} = \frac{[NH_3]_{regeneration}}{[N]_{inflow}} \qquad \text{(Equation 5.4)}$$

$$N_2 \text{ Selectivity} = \frac{[N]_{inflow} - (2[N_2O]+[NH_3]+[NO_x])_{regeneration}}{[N]_{inflow}} \qquad \text{(Equation 5.5)}$$

The trends for the release of NH_3 and N_2O along with NO_x during regeneration at 3% inflow O_2 with 1.7 g of ethanol is demonstrated in Figure 5-9. This trend for NO_x, NH_3, and N_2O is similar for all the test cases. The similar results have been reported in the literature for NH_3 and N_2O with reductants such as H_2, CO and HC [79]. The NH_3 slip downstream of the LNT is observed after the release of NO_x and N_2O. The reductants initially react with released NO_x over an incompletely reduced PGM surface, and therefore N_2O is likely to form at the front part of catalyst [51,52]. The formed NH_3 is transported by convection downstream into the oxidized zone of the catalyst, where it reacts with the stored O_2 and NO_x, delaying the NH_3 slip [51,52].
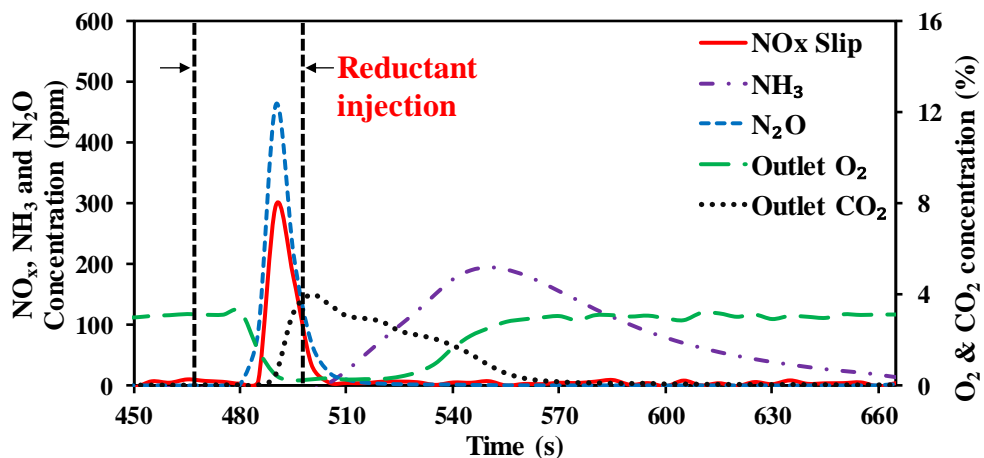
Figure 5-9: NO_x, NH_3 and N_2O trend during regeneration for 1.7 g ethanol at 3% O_2

The NH_3 formation is mainly affected by the presence of H_2 during regeneration [54,55]. The peak value of the NH_3 slip relative to the reductant quantity is shown in Figures 5-10 and 5-11 at the 3% and 8.5% inflow O_2 respectively. The peak NH_3 slip during regeneration is found to be significantly higher with ethanol and n-butanol than with diesel as a reductant. The higher peaks in NH_3 could be because of higher H_2 production with ethanol and n-butanol during the LNT regeneration.
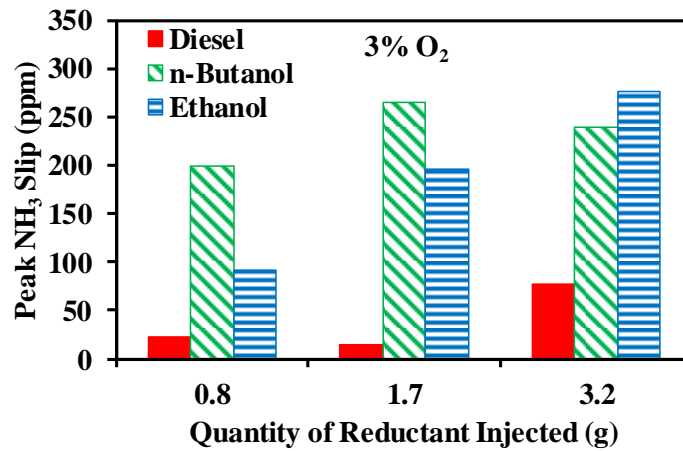
Figure 5-10: Peak NH_3 slip during LNT regeneration at 3% inflow O_2
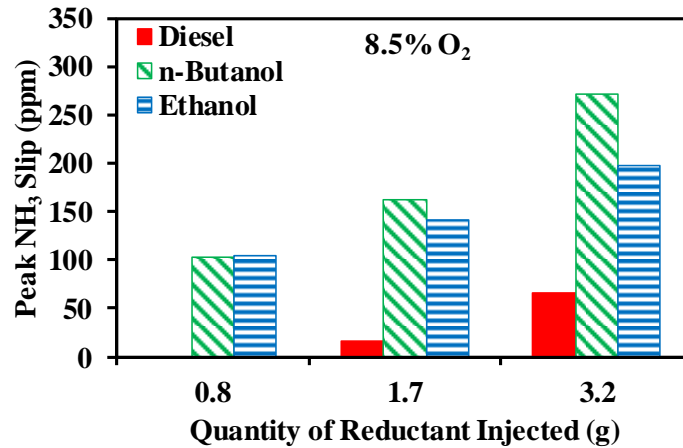
Figure 5-11: Peak NH_3 slip during LNT regeneration at 8.5% inflow O_2

The selectivity towards NH_3 relative to the injected reductant quantity is illustrated in Figures 5.12 and 5.13 at the 3% and 8.5% inflow O_2 respectively. The selectivity towards NH_3 formation increases with the increase in reductant quantity for all tested reductants. The higher NH_3 selectivity is observed with n-butanol and ethanol compared to that of diesel as a reductant. The increase in the selectivity towards NH_3 is ascribed to the higher H_2 concentration during regeneration.
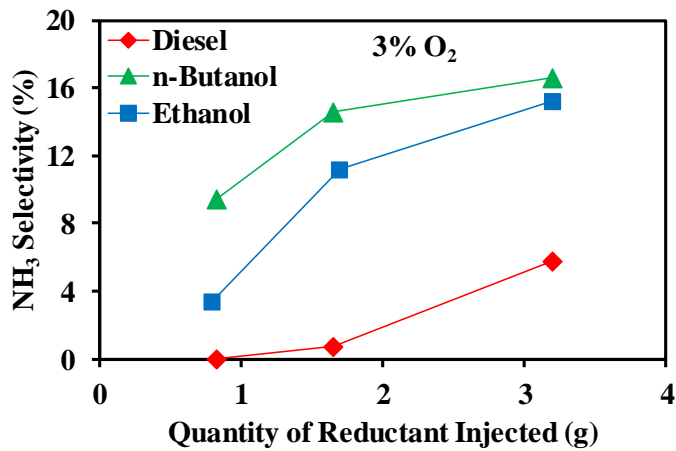
Figure 5-12: Selectivity towards NH_3 at 3% inflow O_2
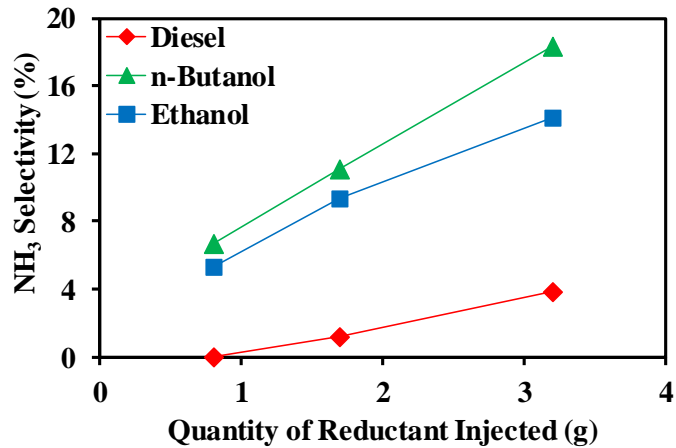
Figure 5-13: Selectivity towards NH_3 at 8.5% inflow O_2

The N_2O is formed by the incomplete reduction of NO_x in the catalyst during regeneration [52]. The peak N_2O slip relative to the reductant quantity of regeneration is represented in Figures 5-14 and 5-15 under the 3% and 8.5% inflow O_2 respectively. At the lowest injected diesel quantity (i.e. 0.8 g), the peak N_2O is lowest, whereas for the higher reductant quantities (i.e. 1.7 g and 3.2 g) the N_2O peak is higher with diesel than with ethanol or n-butanol. The N_2O peak in the ethanol case with 8.5% inflow O_2 decreases with the increase in injected reductant quantity. This could be caused by the enhanced NO_x reduction.
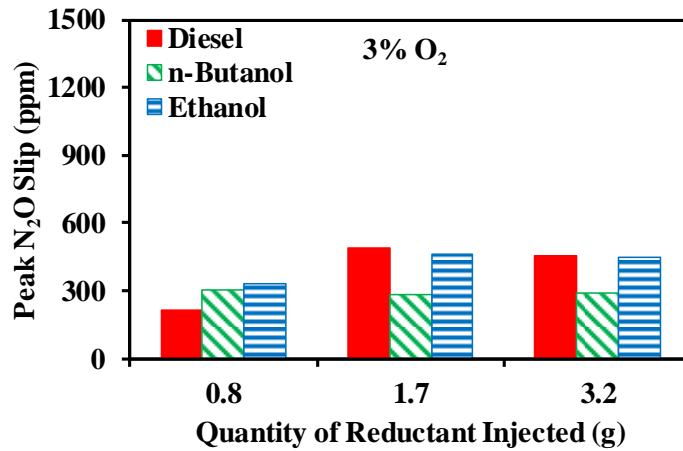
Figure 5-14: Peak N_2O slip during LNT regeneration at 3% inflow O_2
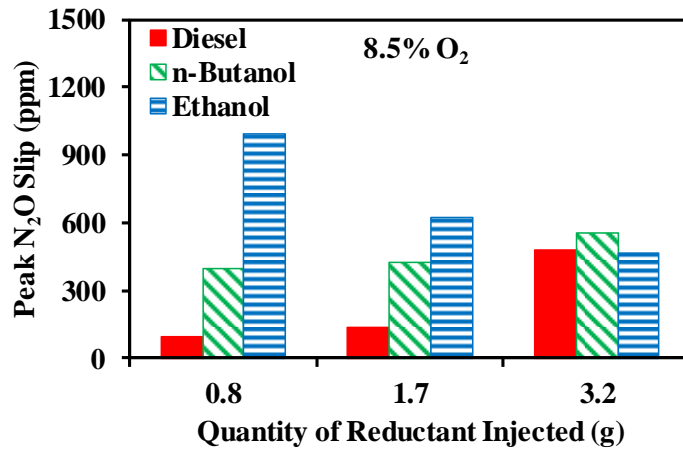
Figure 5-15: Peak N_2O slip during LNT regeneration at 8.5% inflow O_2

The N_2O is a potent greenhouse gas (GHG) and regulated under GHG emission regulations. The instantaneous peak N_2O trend may not correspond to the cumulative N_2O produced during regeneration. The selectivity towards N_2O for all three reductants relative to the injected quantity is shown in Figures 5-16 and 5-17 at the 3% and 8.5% inflow O_2 concentrations respectively. When n-butanol is used as reductant, the selectivity towards N_2O decreased with the increase of the reductant quantity for both inflow O_2 concentrations case. It is also observed that the N_2O selectivity is higher with 8.5% inflow O_2 than with 3% because of higher CO_2 presence, which constraints the effective NO_x conversion [79]. The decrease in the N_2O selectivity with an increase in n-butanol quantity, can further be attributed to the higher reductant reactivity and H_2 yield that helps in improving the NO_x reduction process.
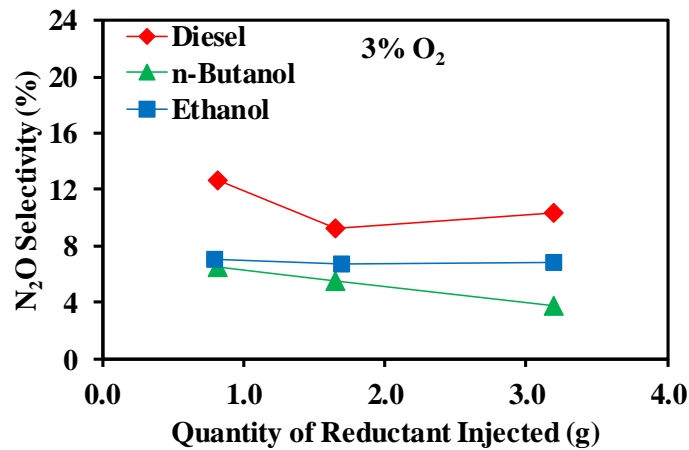
Figure 5-16: Selectivity towards N_2O at 3% inflow O_2

On the contrary, at 8.5% inflow O_2, the selectivity towards N_2O rises with the increase in diesel quantity. The amount of N_2O released using diesel at 3% inflow O_2 is higher than ethanol and n-butanol. The higher N_2O formation observed with diesel at lower O_2 concentration could be caused by the lack of H_2 and CO, which are required for efficient

NO_x conversion. The N_2O selectivity is almost doubled at the lowest quantity (i.e. 0.8 g) of ethanol for 8.5% inflow O_2 compared to 3% case. In the case of ethanol, the selectivity towards N_2O does not change significantly at 3% inflow O_2, whereas the N_2O selectivity decreases to 7% from 15% at 8.5% inflow O_2 with the increase in ethanol quantity.
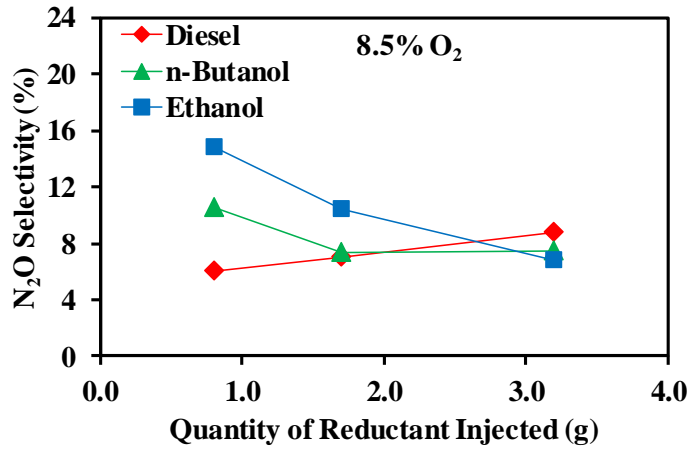
Figure 5-17: Selectivity towards N_2O at 8.5% inflow O_2

An estimation is made for the selectivity towards N_2 during the NO_x conversion. The N_2 selectivity results against the quantity of reductant injected under the 3% and 8.5% inflow O_2 concentration are presented in Figures 5-18 and 5-19 respectively. The selectivity towards N_2 is higher with ethanol as a reductant at 3% inflow O_2. The N_2 selectivity is decreased mainly because of increase in NO_x slip during regeneration. The NO_x is not converted entirely for the lower two quantities (i.e. 0.8 g and 1.7 g) of diesel case at both the inflow O_2 concentration. At 8.5% inflow O_2, regeneration effectiveness is not 100% with 0.8 g and 1.7 g of diesel case (explained in section 5.2.1).
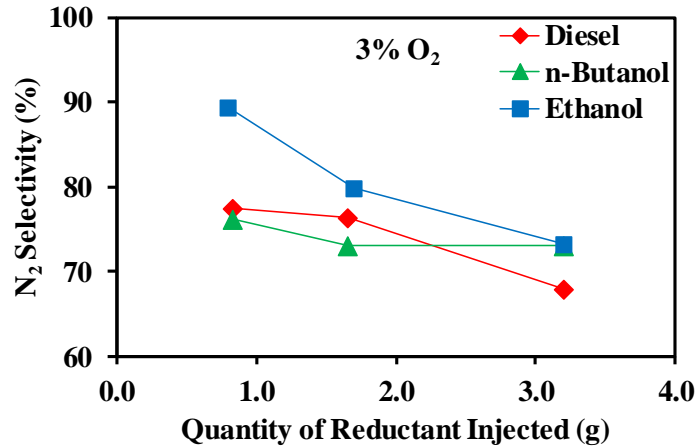
Figure 5-18: Selectivity towards N_2 at 3% inflow O_2
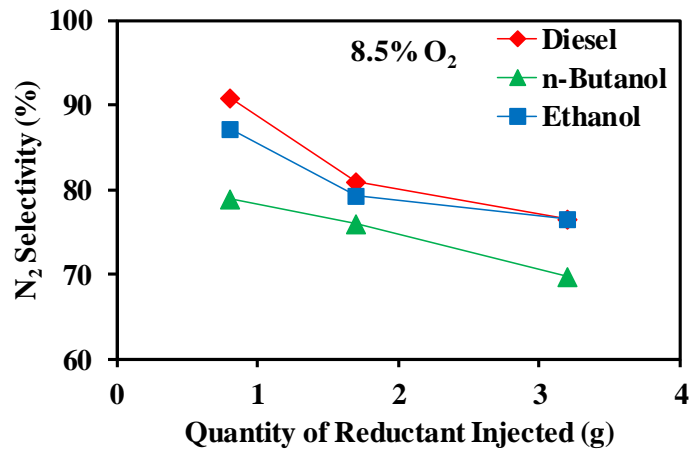
Figure 5-19: Selectivity towards N_2 at 8.5% inflow O_2

5.2.3 Ammonia to NO_x Ratio

The ammonia to NO_x ratio (ANR) is a critical parameter, which affects the NO_x conversion over the SCR convertor. It has been reported in the literature that the ANR before the SCR should be near to 1 for optimal NO_x conversion [34]. Based on the experimental results, molar NH_3 to NO_x ratio is calculated downstream of the LNT catalyst for the reductants used.

The ANR available downstream of the LNT is illustrated in Figures 5-20 and 5-21 at the 3% and 8.5% inflow O_2 respectively. As the reductant quantity increased, more NH_3 formation occurs resulting in an increasing ANR. When ethanol and n-butanol are used as reductants, the ANR is higher than with diesel case because of higher NH_3 concentration. The ANR with n-butanol case increased from 1.2 to 2.5 at 3% inflow O_2 concentration. At the lowest injected quantity (i.e. 0.8 g) of ethanol, NO_x slip is negligible, and by-product (e.g. N_2O and NH_3) formation is significant. Therefore, for the sake of comparison, the ANR is not considered at lowest injected ethanol quantity.
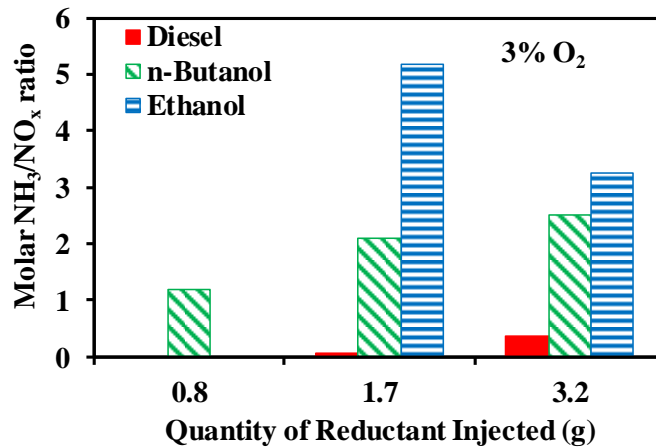
Figure 5-20: Ammonia to NO_x ratio at 3% inflow O_2

With the increase in inflow O_2 concentration from 3 to 8.5%, the ANR is observed to decrease for all the reductants. The ANR is lower with 8.5% inflow O_2 because of less NO_x conversion into NH_3, and more slip of unconverted NO_x during regeneration. The ANR is found to be greater than 1 when 1.7 g and 3.2 g of ethanol and n-butanol is injected at both the inflow O_2 concentrations.
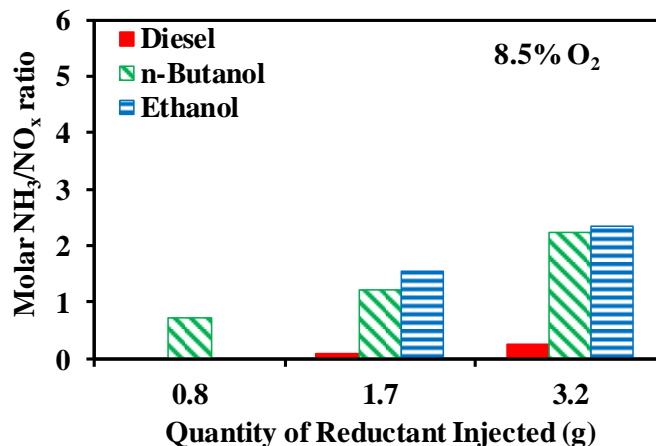
Figure 5-21: Ammonia to NO$_x$ ratio at 8.5% inflow O$_2$

5.2.4 Hydrocarbon Release during LNT Regeneration

The investigation of hydrocarbon (HC) species downstream of the LNT is important in this study to understand the decomposition of a reductant into different HC species. This information will help to understand the reforming and partial oxidation in the LNT catalyst. The ethanol, n-butanol, and diesel reforming in the LNT catalyst can potentially lead to the formation of different HC species. The species concentration during the experiment is measured using the FTIR spectrometer, and the data is analyzed for all the test conditions given in Table 5.1. The variation in HC species concentration is observed with different reductants. The lighter HC (i.e. C$_1$-C$_4$) are dominant species formed with ethanol and n-butanol as reductants. Comparison of the peak concentration of methane (CH$_4$) for all the reductant types is presented in Figure 5-22. Since there are large variations between methane concentrations with the different fuels, the peak methane concentration graph is shown in logarithmic scale. The methane production is significantly higher with ethanol than with diesel and n-butanol as reductants.

58
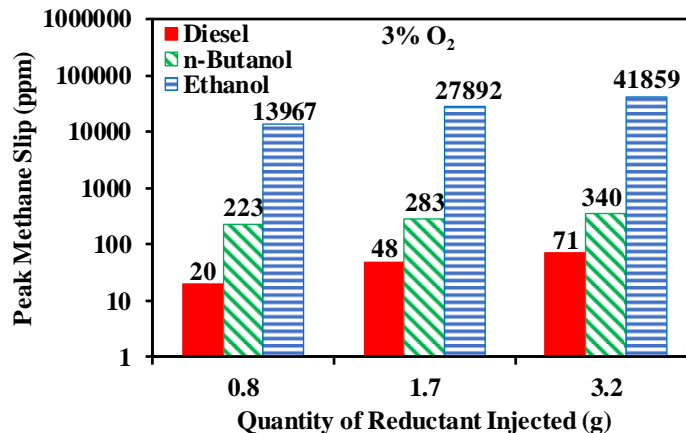
Figure 5-22: Peak methane slip during regeneration at 3% inflow O_2

The peak value of HC species and CO for 1.7 g reductant cases at both the inflow O_2 concentration are demonstrated in Figure 5-23. The methane and CO formation is the highest with ethanol as a reductant. Moreover, aldehydes and propylene are formed in significant amount after the reforming of ethanol and n-butanol as reductants. Among aldehydes family, acetaldehyde is formed with ethanol, whereas butyraldehyde is observed mainly with n-butanol.
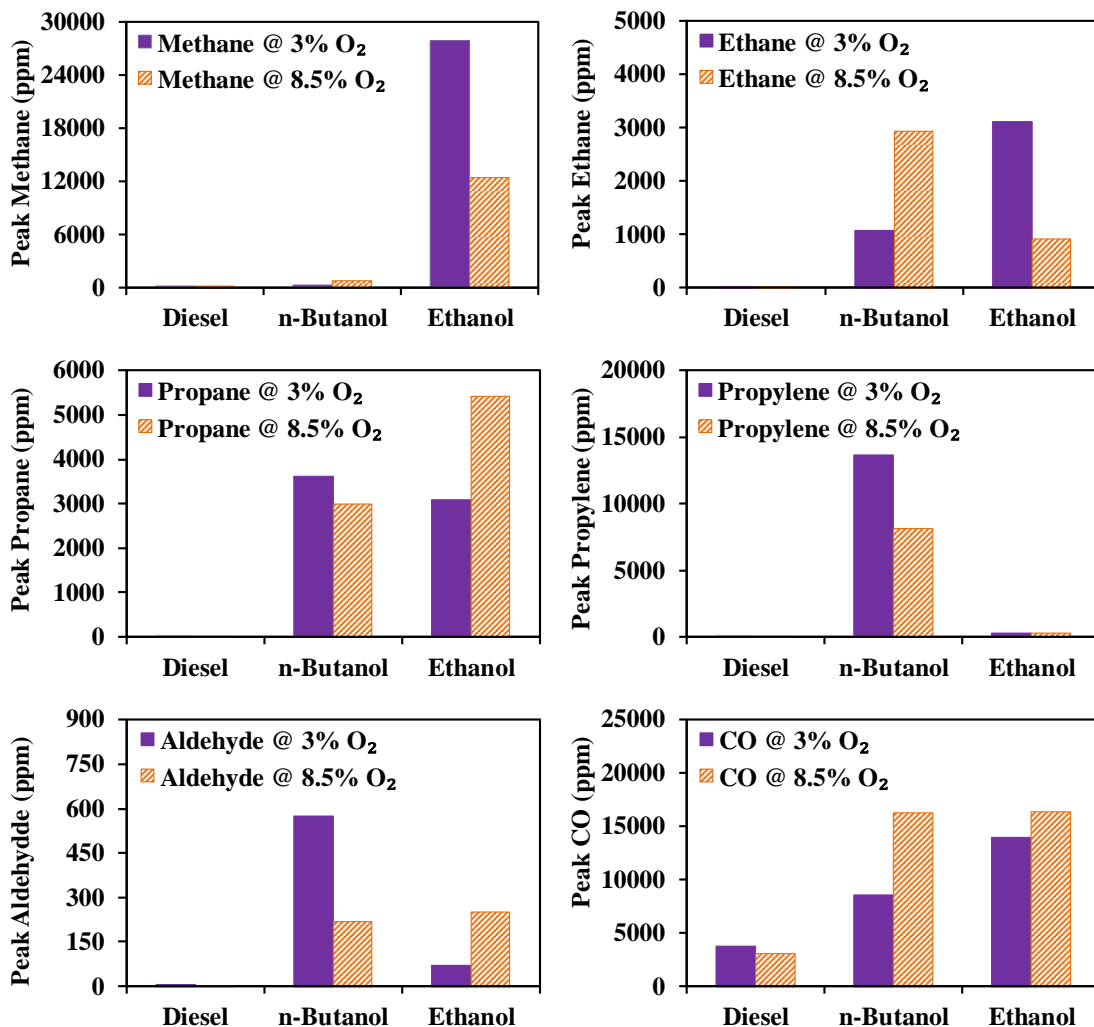
Figure 5-23: Peak HC species and CO at 3% and 8.5% inflow O_2 for all the reductants

The trend for HC species with 1.7 g ethanol under 3% inflow O_2 is shown in Figure 5-24. As the quantity of reductant increases, the release in cumulative amount of HC species also increases. The cumulative amount of methane is significantly higher with the ethanol cases. As a consequence of catalytic reforming, the ethanol decomposition and demethanation during regeneration leads to higher methane formation. The release of HC species for the ethanol cases completes earlier, compared to n-butanol because of its higher volatility. Additionally, the formation of propylene is less with ethanol than with n-butanol as a reductant.
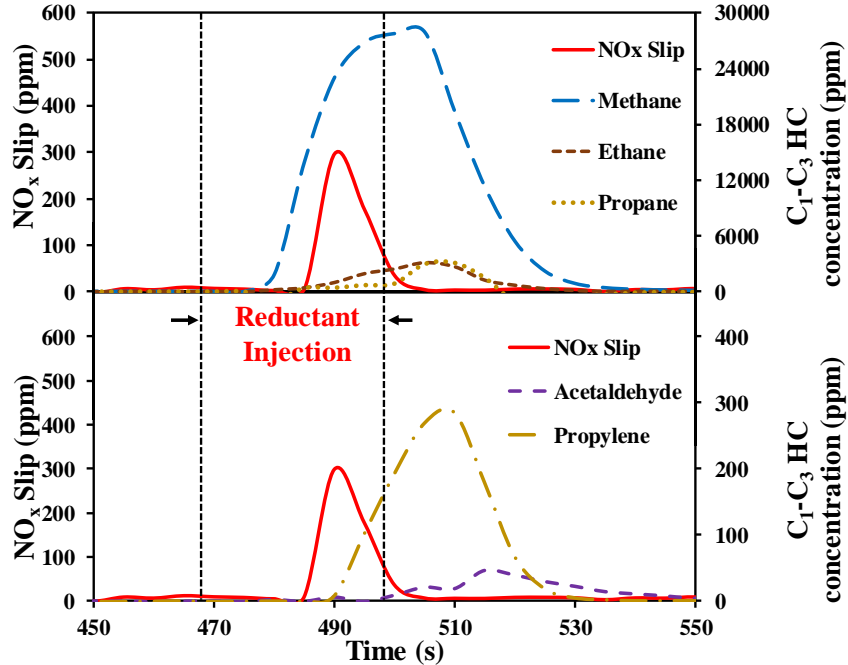
Figure 5-24: HC trend with ethanol as a reductant at 3% inflow O_2

The trend for HC species with 1.7 g n-butanol under 3% inflow O_2 concentration during LNT regeneration is shown in Figure 5-25. The trend for HC species is similar to that of other injected quantities of n-butanol. The cumulative concentration of HC species decreases at higher inflow O_2 level because of enhanced oxidation. The propylene is released a few seconds after the NO_x slip commenced. However, acetaldehyde is released after the completion of reductant injection. The cumulative methane formation during regeneration is significantly less with n-butanol, while the production of propylene is higher than with ethanol and diesel as reductants.

The alkane formation is less significant with n-butanol compared to ethanol case. The higher propylene and aldehyde formation is observed with n-butanol as a reductant. Moreover, the duration of HC slip after the LNT is longer with n-butanol than with ethanol

cases. The propane formation is higher compared to ethane and methane with n-butanol case.
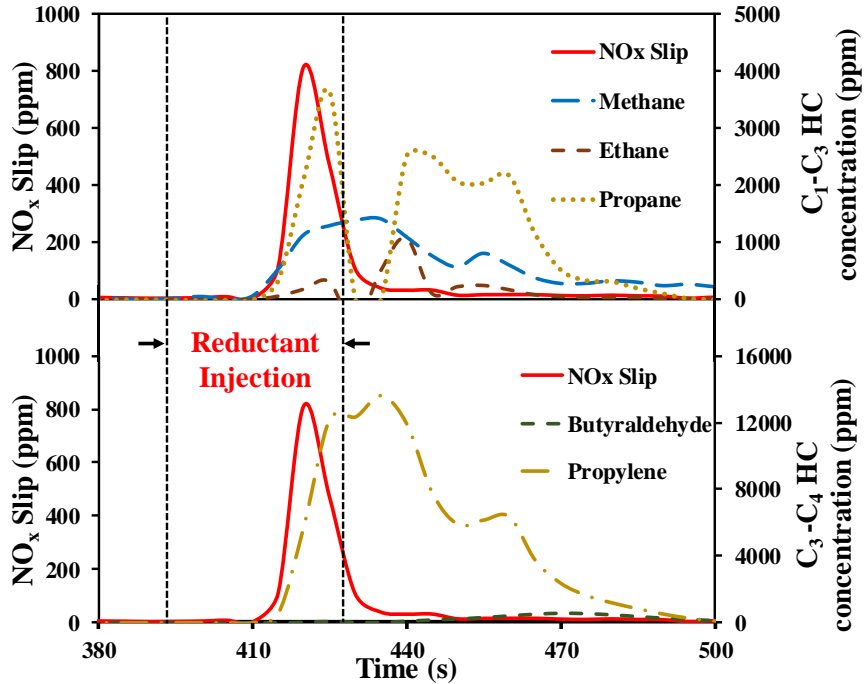
Figure 5-25: HC trend with n-butanol as a reductant at 3% inflow O_2

5.3 Hydrogen Release during Regeneration

The H_2 is the most effective reductant and major constituent affecting NH_3 formation during the LNT regeneration. The H_2 measurement is performed for ethanol and n-butanol as reductants at 3% and 8.5% inflow O_2 concentration. In this research, the reductant is injected before the DOC, which promotes the H_2 reforming because of the precious group metals (Pt, Rh) on the catalyst. The purpose of these experiments is to identify the potential of the H_2 formation using diesel, n-butanol, and ethanol as a reductant to justify NO_x conversion and NH_3 formation during regeneration. The reforming of ethanol and n-butanol starts with the initial dehydrogenation, followed by the rapid release of products such as CH_4, CO_2 and CO.

The test conditions for the H_2 reforming tests are kept similar to the LNT regeneration test conditions, as mentioned in Table 5.1. The separate tests for H_2 reforming are conducted because gas concentration measurement using CAI analyzer, FTIR and H_2 analyzer is difficult at the same time because of the limitation of flow rate on the flow bench setup. The temperature of the catalysts, and injection pressure of water and reductant are kept the same as LNT regeneration tests.

The peak value of H_2 slip relative to the injected quantity of reductant, is demonstrated in Figures 5-26 and 5-27 at the 3% and 8.5% inflow O_2 concentration respectively. The H_2 yield increases with the increase in reductant quantity. The amount of H_2 released after the LNT regeneration is corresponding H_2 that is not utilized in NO_x reduction. The alcohol fuels such as ethanol and n-butanol have higher H/C (hydrogen to carbon ratio), O_2 content, and lower activation energy for breaking the C-C bond. Therefore, the cumulative H_2 yield is higher at low temperature (i.e. 350°C) compared to diesel. The H_2 peak is more for 1.7 g and 3.2 g quantity when ethanol is used as reductant. The higher H_2 peak can be attributed to a lower activation energy for H_2 release from the ethanol during the reforming process in the catalyst. Additionally, the H_2 slip is lower with the lowest injected quantity of ethanol, which could be correlated to the utilization of the H_2 in NO_x conversion. The n-butanol and ethanol require lower temperatures for steam reforming, which may also contribute to the higher production of H_2. The higher H_2 formation during the LNT regeneration leads to the higher NH_3 formation (recall Figures 5-12 and 5-13) as an intermediate product during NO_x reduction on the LNT.
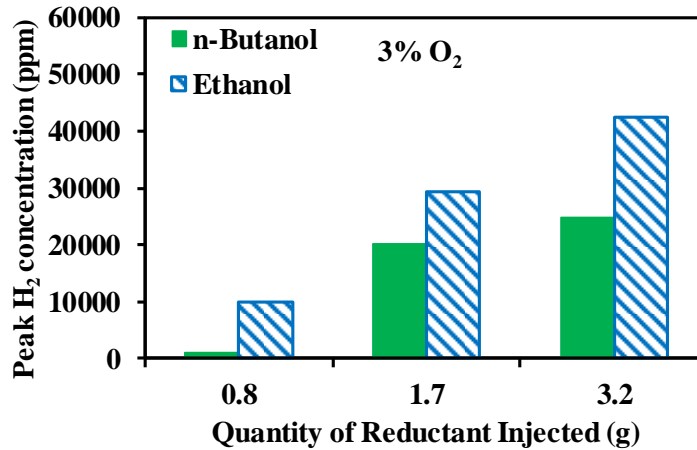
Figure 5-26: Peak H_2 slip during regeneration at 3% inflow O_2
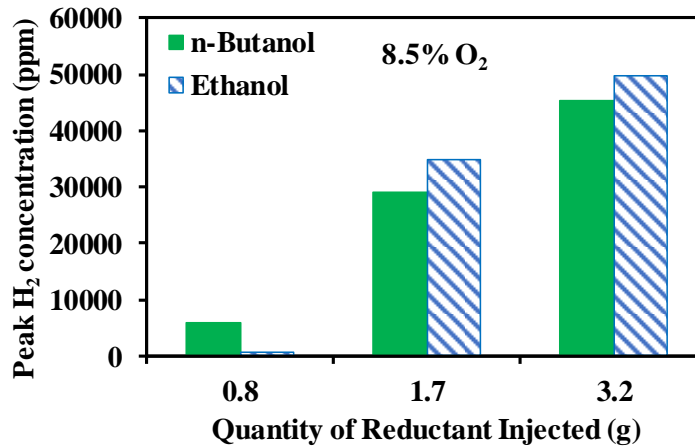
Figure 5-27: Peak H_2 slip during regeneration at 8.5% inflow O_2

The cumulative mass of H_2 slip during the LNT regeneration at the 3% and 8.5% inflow O_2 concentration is shown in Figures 5-28 and 5-29 respectively. Initially, at lower quantity (i.e. 0.8 g) of reductant, it appeared that most of the H_2 formed is utilized in NO_x reduction as well as NH_3 formation. The peak and cumulative amount of H_2 released is highest for 3.2 g of ethanol and n-butanol as reductants. At higher O_2 concentration fast oxidation reaction reduces the H_2 generation. Thus, the cumulative amount of H_2 slip is slightly lower with 8.5% inflow O_2 case than with 3%.

64
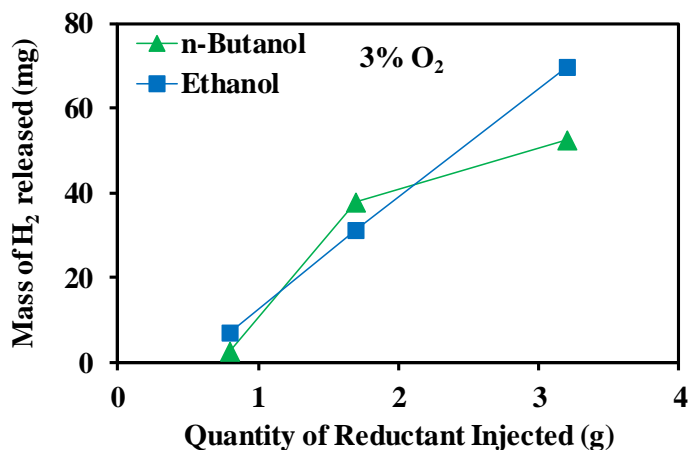
Figure 5-28: Mass of H_2 released during regeneration at 3% inflow O_2
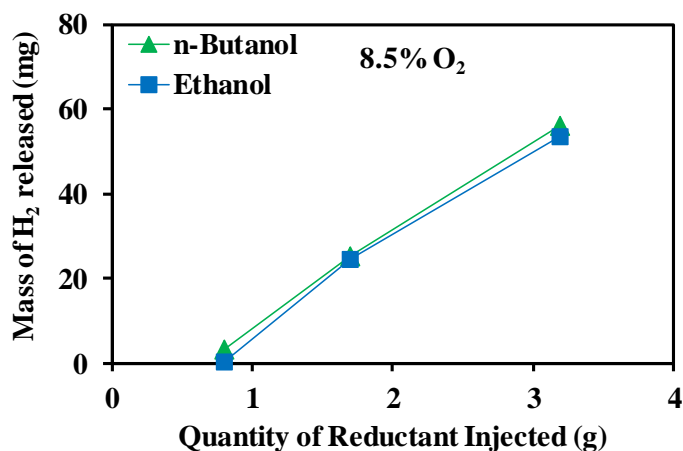
Figure 5-29: Mass of H_2 released during regeneration at 8.5% inflow O_2

5.4 Combined LNT-SCR Investigation

The combined LNT-SCR are performed to investigate the NO_x reduction on the downstream SCR using the generated NH_3 during the LNT regeneration. The combined LNT and SCR experiments are conducted under similar conditions with n-butanol as a reductant for LNT regeneration. It is important to note that urea injection is not used in the experiments. The sampling is required to be implemented before and after the SCR. The gas sampling at both the locations within single LNT regeneration cycle is not possible due

to the limitation of test setup. Therefore, 2 cycles of the LNT regeneration are performed at the same test conditions. Another reason for 2 cycles is that the NH_3 released during first regeneration is adsorbed on the SCR downstream. The absorbed NH_3 utilized for NO_x reduction during 2nd cycle of regeneration. In the previous experiments, sufficient ammonia to NO_x ratio is observed with 1.7 g of n-butanol at 3% inflow O_2 (see Figure 5-20). The test conditions for the LNT- SCR are presented in table

Table 5.2 Combined LNT-SCR test conditions

Reductant	LNT Temp (°C)	SCR Temp (°C)	NO_x Stored (g)	Reductant Quantity (g)	O_2 (%)	H_2O (%)
n-Butanol	350	265	0.21	1.7	3	6

During the 1st cycle of LNT regeneration sampling for FTIR is done before the SCR. The trend for NO_x, NH_3, N_2O, and NO_2 before the SCR is shown in Figure 5-30. The peak NO_x, N_2O, NH_3 and NO_2 measured before the SCR are 378, 252, 532 and 9 ppm respectively.
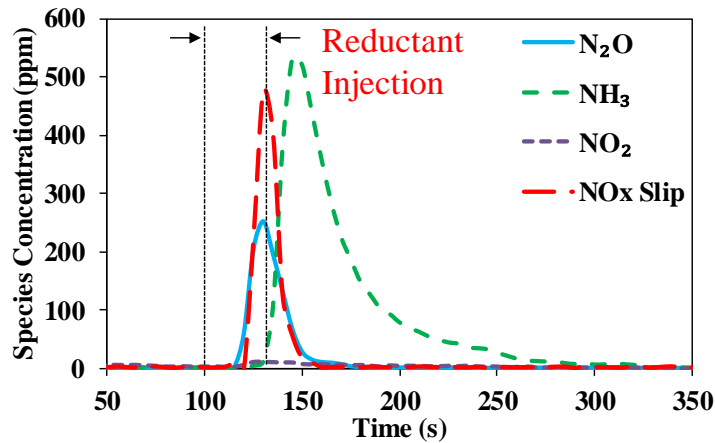
Figure 5-30: Nitrogen-based species before SCR during LNT regeneration (1st cycle)

During the 2nd cycle of LNT regeneration, FTIR sampling is done after the SCR. The trend for N_2O, NH_3, NO_2 and NO_x after the SCR is shown in Figure 5-31. Most of the NH_3

formed during regeneration is absorbed on the downstream SCR. The NO_x peak is observed to be slightly lower than the previous cycle. However, there is no significant reduction in the cumulative quantity of NO_x is observed compared to the 1st cycle of regeneration after the SCR. Therefore, in the tested cases, no effect of the Cu-SCR convertor is observed on further NO_x reduction after the LNT catalyst. This could be attributed to the lower SCR temperature for reaction to occur, and the HC fouling on the active sites of SCR.
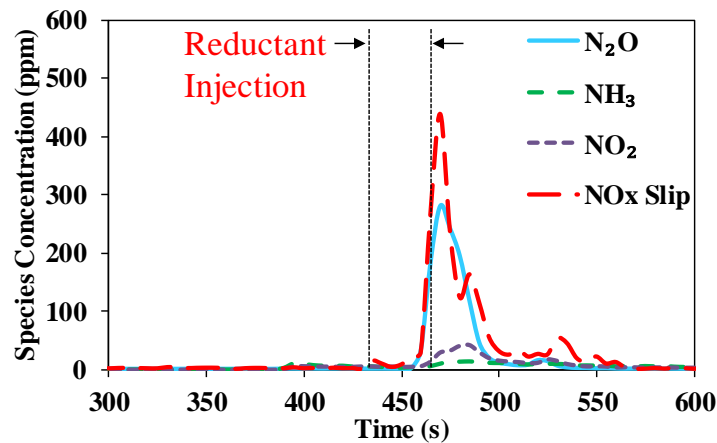
Figure 5-31: Nitrogen-based species after SCR during LNT regeneration (2nd cycle)

To determine the HC absorption on the SCR, an investigation of the HC species before and after the SCR is performed. Researchers have reported that HC deposition can affect the NO_x reduction activity on the SCR [80]. Therefore, HC species based on the FTIR data are analyzed for the same experiment. The trend for different HC before and after the SCR is presented in Figures 5-32 and 5-33 respectively. There is not significant change observed in the methane concentration across the SCR. The concentrations of ethane and propane are decreased after the SCR. When sampling is implemented after the LNT catalyst, high concentration (~2500 ppm) of propylene is observed with 1.7 g of n-butanol as reductant, as shown in Figure 5-32. However, propylene concentration is observed to be significantly

less after the SCR as shown in Figure 33. Similarly, butyraldehyde after the SCR is not detected. The duration of the breakthrough for HC species and NO_x after the SCR is longer than after the LNT catalyst. Overall, a significant change in the HC concentration before and after the SCR is found that indicates HC fouling on the SCR surface when n-butanol is used a reductant for the LNT regeneration. The absorbed HC species on the active sites of the Cu-SCR surface negatively affects the NO_x conversion reaction. The experiment is repeated at the same conditions, but similar trends are observed with n-butanol as a reductant.
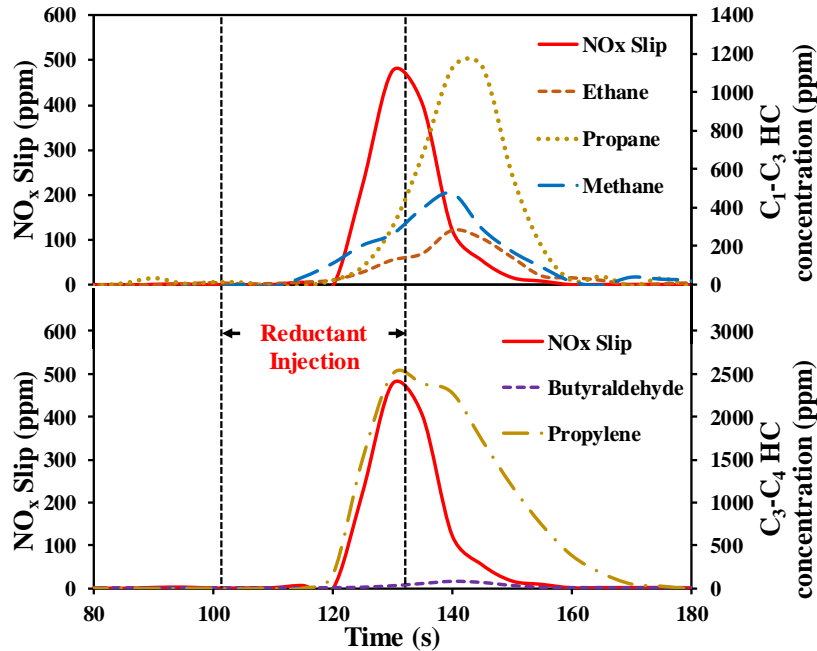
Figure 5-32: HC species before SCR during LNT regeneration (1st cycle)
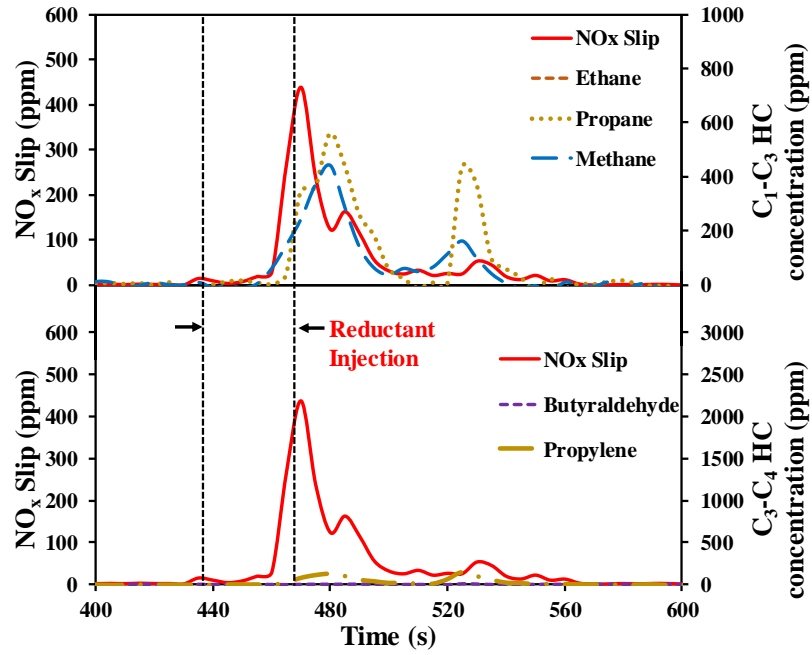
Figure 5-33: HC species after SCR during LNT regeneration (2nd cycle)

CHAPTER 6:   CONCLUSIONS

This chapter provides a summary of the main results based on the experimental investigation, along with conclusions derived from the results. The limitations and future recommendations related of work are also discussed. Initially, the engine test results at the medium load using diesel, n-butanol, and ethanol-diesel are discussed to demonstrate the exhaust conditions suitable for the long breathing LNT operation. Then the LNT regeneration tests are performed under engine exhaust like conditions on an offline after-treatment test bench. To fulfill the objective of the after-treatment tests, the alcohol fuels such as ethanol and n-butanol are used as a reductant, for the LNT regeneration. In the end, the combined LNT-SCR after-treatment system is tested using n-butanol as a reductant for the LNT regeneration. The conclusion based on the experimental investigations are summarized below:

Engine Test Results

- With the application of EGR, the engine-out NO_x and PM emissions are observed to be within a sufficiently low range that is suitable for the long breathing LNT operations at the medium engine load with n-butanol DI.

- The ethanol diesel dual-fuel combustion with the application of moderate EGR can achieve low NO_x and PM emissions. At medium engine load, suitable ranges of NO_x and PM emissions are achieved for the long breathing LNT operations. However, higher CO and THC emissions are observed.

LNT Regeneration

- The regeneration effectiveness is higher when ethanol and n-butanol are used as reductants, because the NO_x slip is less observed during the purge period compared to diesel operations with 3% and 8.5% inflow O_2 concentrations.

- The use of ethanol is proved to be a better reductant for NO_x reduction over the LNT catalyst, because less amount of NO_x slip per mass of NO_x stored is observed compared to n-butanol and diesel for the 3% and 8.5% inflow O_2 operations under an average LNT temperature of ~350°C. The higher NO_x conversion is achieved in part, by the higher H_2 yield during regeneration, and the higher volatility of ethanol, as a reductant.

- The NH_3 formation is higher with ethanol and n-butanol than with diesel during the LNT regeneration. The ammonia to NO_x ratio (ANR) is the highest with ethanol as a reductant.

- The selectivity towards N_2O decreased with the increase in injected quantity with ethanol and n-butanol as reductants due to better NO_x conversion in presence of higher H_2 and CO during the LNT regeneration under the bench testing conditions.

- The hydrogen yield by the reforming effect of ethanol and n-butanol in the catalyst, is significantly higher compared to using diesel. The availability of H_2 before the LNT catalyst is effective to increase the NO_x reduction and the ammonia formation during regeneration.

- The concentration of lighter HC (C_1-C_4) species is higher downstream of the LNT with ethanol and n-butanol compared to using diesel as a reductant. The methane (greenhouse gas) formation is higher with ethanol as a reductant.

- The combined LNT-SCR after-treatment shows no significant change in overall NO_x reduction with n-butanol as a reductant at the tested conditions.

Additional Remarks and Future Works

- Investigations are required to determine whether the long breathing LNT operation requirements can be achieved at high load conditions for different fuelling methods (diesel DI, n-butanol DI and ethanol PFI-diesel DI) with EGR.
- Further LNT regeneration tests should be performed with more variations in testing conditions (e.g. temperature, space velocity, regeneration duration, reductant types, and O_2 concentration). Other reducing agents such as DME and gasoline, should be investigated, in comparison with diesel, n-butanol and ethanol as reductants.
- The LNT regeneration performance should be further investigated directly with the actual engine exhaust.
- The combined LNT-SCR should be tested more with other reducing agents, and to utilize NH_3 generated during the LNT regenerations over a subsequent SCR convertor for further NO_x reductions.

REFERENCES

1. Heywood, J.B., "Internal Combustion Engine Fundamentals", McGraw-Hill Singapore, 1998.

2. Stone R, "Introduction to Internal Combustion Engines", 3rd Edition, Macmillan, 1999.

3. Robert Bosch GmbH, "Diesel-Engine Management," 3rd Edition, SAE International, ISBN 0-13: 0-7680-1343-7, 2004.

4. The impact of vehicle and fuel standards on premature mortality and emissions | International Council on Clean Transportation, https://www.theicct.org/publications/impact-vehicle-and-fuel-standards-premature-mortality-and-emissions, Nov. 2018.

5. Asad, U., "Advanced diagnostics, control and testing of diesel low temperature combustion," PhD Dissertations, 2014.

6. Johnson, T., "Diesel Emissions in Review," SAE Int. J. Engines 4(1):143-157, 2011,

7. EPA Emission Standards for Heavy-Duty Highway Engines and Vehicles, https://www.epa.gov/emission-standards-reference-guide/epa-emission-standards-heavy-duty-highway-engines-and-vehicles, Nov.2018

8. Emission Standards: Europe: Heavy-Duty Truck and Bus Engines, https://www.dieselnet.com/standards/eu/hd.php, Oct. 2018.

9. Ladommatos, N., Abdelhalim, S.M., Zhao, H., and Hu, Z., "The Dilution, Chemical, and Thermal Effects of Exhaust Gas Recirculation on Diesel Engine Emissions - Part 2: Effects of Carbon Dioxide," 1996.

10. Ladommatos, N., Abdelhalim, S.M., Zhao, H., and Hu, Z., "The Dilution, Chemical, and Thermal Effects of Exhaust Gas Recirculation on Disesel Engine Emissions - Part 4: Effects of Carbon Dioxide and Water Vapour," 1997.

11. Kreso, A., Johnson, J., Gratz, L., Bagley, S. *et al*., "A Study of the Effects of Exhaust Gas Recirculation on Heavy-Duty Diesel Engine Emissions," SAE Technical Paper 981422, 1998.

12. Zheng, M., Reader, G.T., and Hawley, J.G., "Diesel engine exhaust gas recirculation––a review on advanced and novel concepts," Energy Conversion and Management 45(6):883–900, 2004.

13. Asad, U., Tjong, J., and Zheng, M., "Exhaust gas recirculation – Zero dimensional modelling and characterization for transient diesel combustion control," Energy Conversion and Management 86:309–324, 2014.

14. Zheng, M., Asad, U., Reader, G.T., Tan, Y. *et al*., "Energy efficiency improvement strategies for a diesel engine in low-temperature combustion," International Journal of Energy Research 33(1):8–28, 2009.

15. Benson R.S. and Whitehouse N.D., 1979, "Internal Combustion Engines", Pergamon Press.

16. de Ojeda, W., Bulicz, T., Han, X., Zheng, M. *et al*., "Impact of Fuel Properties on Diesel Low Temperature Combustion," SAE Int. J. Engines 4(1):188-201, 2011.

17. Alriksson, M. and Denbratt, I., "Low Temperature Combustion in a Heavy Duty Diesel Engine Using High Levels of EGR," SAE Technical Paper 2006-01-0075, 2006.

18. Han, X.,"Study of fuels and fuelling strategies for enabling clean combustion in compression ignition engines," Electronic Theses and Dissertations, 2014.

19. Ogawa, H., Miyamoto, N., Shimizu, H., and Kido, S., "Characteristics of Diesel Combustion in Low Oxygen Mixtures with Ultra-High EGR," SAE Technical Paper 2006-01-1147, 2006.

20. Zheng, M., Asad, U., Kumar, R., Reader, G. *et al*., "An Investigation of EGR Treatment on the Emission and Operating Characteristics of Modern Diesel Engines", SAE Technical Paper 2007-01-1083, 2007.

21. Dronniou, N., Lejeune, M., Balloul, I., and Higelin, P., "Combination of High EGR Rates and Multiple Injection Strategies to Reduce Pollutant Emissions," SAE Technical Paper 2005-01-3726, 2005.

22. Idicheria, C. and Pickett, L., "Soot Formation in Diesel Combustion under High-EGR Conditions," SAE Technical Paper 2005-01-3834, 2005.

23. Wang, M., Han, J., Dunn, J.B., Cai, H. *et al*., "Well-to-wheels energy use and greenhouse gas emissions of ethanol from corn, sugarcane and cellulosic biomass for US use," Environ. Res. Lett. 7(4):045905, 2012.

24. IEA - Brazil, https://www.iea.org/policiesandmeasures/pams/brazil/name-140350-en.php, Nov. 2018.

25. Almost all U.S. gasoline is blended with 10% ethanol - Today in Energy - U.S. Energy Information Administration (EIA), https://www.eia.gov/todayinenergy/detail.php?id=26092, Nov. 2018.

26. Yanai, T., Dev, S., Han, X., Zheng, M. *et al.*, "Impact of Fuelling Techniques on Neat n-Butanol Combustion and Emissions in a Compression Ignition Engine," SAE International Journal of Engines 8(2):735–746, 2015.

27. Gao, T., Divekar, P., Asad, U., Han, X. *et al.*, "An Enabling Study of Low Temperature Combustion With Ethanol in a Diesel Engine," J. Energy Resour. Technol 135(4):042203-042203–8, 2013.

28. Russell, A. and Epling, W.S., "Diesel Oxidation Catalysts," *Catalysis Reviews* 53(4):337–423, 2011.

29. Lizarraga, L., Souentie, S., Boreave, A., George, C. *et al.*, "Effect of diesel oxidation catalysts on the diesel particulate filter regeneration process," *Environ. Sci. Technol.* 45(24):10591–10597, 2011.

30. Guan, B., Zhan, R., Lin, H., and Huang, Z., "Review of the state-of-the-art of exhaust particulate filter technology in internal combustion engines," *J. Environ. Manage.* 154:225–258, 2015.

31. Seo, J., Park, W., and Lee, M., "The Best Choice of Gasoline/Diesel Particulate Filter to Meet Future Particulate Matter Regulation," SAE Technical Paper 2012-01-1255, 2012.

32. MECA, 2005. "Diesel Particulate Filter Maintenance: Current Practices and Experience", Manufacturers of Emission Controls Association, Washington, D.C., June 2005,

33. Koebel, M., Elsener, M., and Kleemann, M., "Urea-SCR: a promising technique to reduce NO_x emissions from automotive diesel engines," *Catalysis Today* 59(3):335–345, 2000.

34. Nova, I. and Tronconi, E., "Urea-SCR Technology for deNOx After Treatment of Diesel Exhausts," Springer-Verlag, New York, ISBN 978-1-4899-8070-0, 2014.

35. Liu, Y., Liu, Z., Mnichowicz, B., Harinath, A.V. *et al.*, "Chemical deactivation of commercial vanadium SCR catalysts in diesel emission control application," Chemical Engineering Journal 287:680–690, 2016.

36. Cheng, Y., Montreuil, C., Cavataio, G., and Lambert, C., "The Effects of SO_2 and SO_3 Poisoning on Cu/Zeolite SCR Catalysts," SAE Technical Paper 2009-01-0898, 2009

37. Guo, G., Dobson, D., Warner, J., Ruona, W. *et al.*, "Advanced Urea SCR System Study with a Light Duty Diesel Vehicle," SAE Technical Paper 2012-01-0371, 2012.

38. Ramsbottom, M., Birkby, N., Khadiya, N., and Beesley, S., "Development of a Thermal Enhancer™ for Combined Partial Range Burning and Hydrocarbon Dosing on Medium and Heavy Duty Engine Applications," SAE Technical Paper 2011-01-0298, 2011.

39. Takeshima, S., Tanaka, T., Iguchi, S., Araki, Y. *et al.*, "Exhaust purification device of internal combustion engine," US5437153A, 1995.

40. Takahashi, N., Yamazaki, K., Sobukawa, H., and Shinjoh, H., "The low-temperature performance of NO_x storage and reduction catalyst," Applied Catalysis B: Environmental 70(1):198–204, 2007.

41. Hachisuka, I., Hirata, H., Ikeda, Y., and Matsumoto, S., "Deactivation Mechanism of NO_x Storage-Reduction Catalyst and Improvement of Its Performance," SAE Technical Paper 2000-01-1196, 2000.

42. NO$_x$ control technologies for Euro 6 diesel passenger cars | International Council on Clean Transportation, https://www.theicct.org/publications/nox-control-technologies-euro-6-diesel-passenger-cars, Nov. 2018.

43. Ojeda, W. de, Zheng, M., Han, X., Jeftic, M. *et al.*, "Diesel Engine NO$_x$ Reduction," US20150113961A1, 2015.

44. Jeftic, M., "Strategies for Enhanced After-Treatment Performance: Post Injection Characterization and Long Breathing with Low NO$_x$ Combustion," Electronic Theses and Dissertations, 2016.

45. Aversa, C., "Investigation on the Performance of a Long Breathing Lean NO$_x$ Trap Using n-Butanol". Electronic Theses and Dissertations, 2017.

46. Liu, G. and Gao, P.-X., "A review of NO$_x$ storage/reduction catalysts: mechanism, materials and degradation studies," Catal. Sci. Technol. 1(4):552–568, 2011.

47. Olsson, L., Persson, H., Fridell, E., Skoglundh, M. *et al.*, "A Kinetic Study of NO Oxidation and NO$_x$ Storage on Pt/Al$_2$O$_3$ and Pt/BaO/Al$_2$O$_3$," J. Phys. Chem. B 105(29):6895–6906, 2001.

48. Olsson, L., Blint, R.J., and Fridell, E., "Global Kinetic Model for Lean NO$_x$ Traps," Ind. Eng. Chem. Res. 44(9):3021–3032, 2005.

49. Bhatia, D., Clayton, R.D., Harold, M.P., and Balakotaiah, V., "A global kinetic model for NO$_x$ storage and reduction on Pt/BaO/Al$_2$O$_3$ monolithic catalysts," Catalysis Today 147:S250–S256, 2009.

50. Fridell, E., Skoglundh, M., Westerberg, B., Johansson, S. *et al.*, "NO$_x$ Storage in Barium-Containing Catalysts," Journal of Catalysis 183(2):196–209, 1999.

51. Bhatia, D., Harold, M.P., and Balakotaiah, V., "Modeling the effect of Pt dispersion and temperature during anaerobic regeneration of a lean NO_x trap catalyst," *Catalysis Today* 151(3):314–329, 2010.

52. Xue, E., Seshan, K., and Ross, J.R.H., "Roles of supports, Pt loading and Pt dispersion in the oxidation of NO to NO_2 and of SO_2 to SO_3," *Applied Catalysis B: Environmental* 11(1):65–79, 1996.

53. Lindholm, A., Currier, N.W., Fridell, E., Yezerets, A. *et al.*, "NO_x storage and reduction over Pt based catalysts with hydrogen as the reducing agent: Influence of H_2O and CO_2," *Applied Catalysis B: Environmental* 75(1):78–87, 2007.

54. Maurer, M., Holler, P., Zarl, S., Fortner, T. *et al.*, "Investigations of Lean NO_x Trap (LNT) Regeneration Strategies for Diesel Engines," SAE Technical Paper 2017-24-0124, 2017.

55. Kočí, P., Bártová, Š., Mráček, D., Marek, M. *et al.*, "Effective Model for Prediction of N_2O and NH_3 Formation During the Regeneration of NO_x Storage Catalyst," Top Catal 56(1):118–124, 2013.

56. Mráček, D., Kočí, P., Marek, M., Choi, J.-S. *et al.*, "Dynamics of N_2 and N_2O peaks during and after the regeneration of lean NO_x trap," Applied Catalysis B: Environmental 166–167:509–517, 2015.

57. Kubiak, L., Matarrese, R., Castoldi, L., Lietti, L. *et al.*, "Study of N_2O Formation over Rh- and Pt-Based LNT Catalysts," *Catalysts* 6(3):36, 2016.

58. Castoldi, L., Lietti, L., Forzatti, P., Morandi, S. *et al.*, "The NO_x storage-reduction on PtK/Al_2O_3 Lean NO_x Trap catalyst," Journal of Catalysis 276(2):335–350, 2010.

59. Artioli, N., Matarrese, R., Castoldi, L., Lietti, L. *et al.*, "Effect of soot on the storage-reduction performances of PtBa/Al$_2$O$_3$ LNT catalyst," *Catalysis Today* 169(1):36–44, 2011.

60. Lindholm, A., Currier, N.W., Dawody, J., Hidayat, A. *et al.*, "The influence of the preparation procedure on the storage and regeneration behavior of Pt and Ba based NO$_x$ storage and reduction catalysts," Applied Catalysis B: Environmental 88(1):240–248, 2009.

61. Castoldi, L., Nova, I., Lietti, L., and Forzatti, P., "Study of the effect of Ba loading for catalytic activity of Pt–Ba/Al$_2$O$_3$ model catalysts," *Catalysis Today* 96(1):43–52, 2004.

62. Cheekatamarla, P.K. and Finnerty, C.M., "Reforming catalysts for hydrogen generation in fuel cell applications," *Journal of Power Sources* 160(1):490–499, 2006

63. Bion, N., Epron, F., and Duprez, D., "Bioethanol reforming for H$_2$ production. A comparison with hydrocarbon reforming," Catalysis, 1–55, 2010.

64. Nahar, G.A. and Madhani, S.S., "Thermodynamics of hydrogen production by the steam reforming of butanol: Analysis of inorganic gases and light hydrocarbons," *International Journal of Hydrogen Energy* 35(1):98–109, 2010.

65. Gutierrez, A., Karinen, R., Airaksinen, S., Kaila, R. *et al.*, "Autothermal reforming of ethanol on noble metal catalysts," *International Journal of Hydrogen Energy* 36(15):8967–8977, 2011.

66. Wang, J., Ji, Y., He, Z., Crocker, M. *et al.*, "A non-NH$_3$ pathway for NO$_x$ conversion in coupled LNT-SCR systems," *Applied Catalysis B: Environmental* 111–112:562–570, 2012.

67. Chimner, C., "Transient On-Road Emission Reduction of an LNT + SCR Aftertreatment System," *SAE International Journal of Commercial Vehicles* 1(1):315–326, 2008.

68. Gough, B., Kotrba, A., Salanta, G., Popovich, J. *et al*., "Transient Performance of an HC LNC Aftertreatment System Applying Ethanol as the Reductant," SAE Technical Paper 2012-01-1957, 2012.

69. Wittka, T., Holderbaum, B., Dittmann, P., and Pischinger, S., "Experimental Investigation of Combined LNT + SCR Diesel Exhaust Aftertreatment," Emiss. Control Sci. Technol. 1(2):167–182, 2015.

70. Gurley Precision Instruments, "Gurley Series 9X25 Rotary Incremental Encoders", 2006, 606.

71. Gao, T., "Mixing and Reactivity Control with Butanol and Ethanol in Compression Ignition Engines," Electronic Theses and Dissertations, 2017.

72. Lapuerta, M., Contreras, R., Fernadez, J., Dorado, M., "Stability, Lubricity, Viscosity, and Cold-Flow Properties of Alcohol-Diesel Blends," Energy Fuels 2010, 24, 4497–4502.

73. Sigma-Alorich, "1-Butanol, HPLC grade", http://www.sigmaaldrich.com/catalog/product/sigald/34867?lang=en&region=CA, Nov. 2018

74. Sigma-Alorich, " Ethyl alcohol, Pure, Anhydrous", http://www.sigmaaldrich.com/catalog/product/sial/459836?lang=en&region=CA, Nov. 2018

75. MKS Instruments, "MKS Type MultiGas™ Analyzer Models 2030, 2031 and 2032 Hardware Manual", 2006, 134987-P1 Rev B 09/06.

76. V&F Analyse und Messtechnik Ges.M.B.H Instrumentation and Environmental Technology, "Technical Description Hydrogen Monitoring System", 2005, Version 2/02.

77. Yu, S., Dev, S., Yang, Z., Leblanc, S. *et al.*, "Early Pilot Injection Strategies for Reactivity Control in Diesel-ethanol Dual Fuel Combustion," SAE Technical Paper 2018-01-0265, 2018.

78. Epling, W.S., Campbell, G.C., and Parks, J.E., "The Effects of CO_2 and H_2O on the NO_x Destruction Performance of a Model NO_x Storage/Reduction Catalyst," Catalysis Letters 90(1):45–56, 2003.

79. Zhu, J., Shen, M., Wang, J., Wang, X. *et al.*, "N_2O formation during NO_x storage and reduction using C3H6 as reductant," Catalysis Today 297:92–103, 2017.

80. Malpartida, I., Marie, O., Bazin, P., Daturi, M. *et al.*, "An operando IR study of the unburnt HC effect on the activity of a commercial automotive catalyst for NH_3-SCR," Applied Catalysis B: Environmental 102(1):190–200, 2011.

VITA AUCTORIS

NAME:	Divyanshu Purohit
PLACE OF BIRTH:	Barmer, Rajasthan, India
YEAR OF BIRTH:	1993
EDUCATION:	Bachelor of Engineering (Automobile Engineering)
	Rajiv Gandhi Technological University, India
	2010-2014
	M.A.Sc. Mechanical Engineering
	University of Windsor, Canada
	2016-2018